MIE versus CIE: Comparative Analysis of Magnetic and Classical Isotope Effects

Anatoly L. Buchachenko

Institute of Chemical Physics, 4 Kosygin Street, Moscow 117977, Russia

Received March 16, 1994 (Revised Manuscript Received June 20, 1995)

Contents

I. Introduction

Spin chemistry as a new field of chemical science is based on the fundamental principle: *chemical reactions are spin selective; they are allowed only for such spin states of products whose total electron spin is identical to that of reagents and are forbidden if they require a change of spin.* Only magnetic interactions are able to change the spin of reactive intermediates and transform their nonreactive, spin-forbidden states into the reactive, spin-allowed ones. Contributing nothing to the chemical energy, magnetic interactions switchover the reaction from the spin-closed channels to the spin-open ones (or *vice versa*, depending on the starting spin state of reagents).[1] Ultimately, they modify chemical reactivity and write a new, *magnetic scenario of chemical reaction.*

Being *electron spin selective*, the chemical interaction between the spin-carrying chemical species (radicals, for instance) is also inevitably *nuclear spin selective.* If both electron and nuclear spin subsystems are coupled by the Fermi, or hyperfine magnetic interaction (HFI), then the nuclear spin subsystem can affect the behavior of the electron spin subsystem through HFI and, hence, modify the chemical reactivity. The *nuclear spin selectivity* differentiates the reaction rates for radicals (or, in general, for any other spin-bearing chemical species) with magnetic and nonmagnetic isotopic nuclei. This new phenomenon[2] is the *magnetic isotope effect* (MIE), in contrast to the well-known *classical isotope effect* (CIE) which is the consequence of the *nuclear mass selectivity* of chemical reactions.

Anatoly L. Buchachenko was born in Russia in 1935. He graduated from Gorki (Nizhny Novgorod) State University in 1958. Currently he is a Professor at the Moscow State University and Director of the Institute of Chemical Physics. His interests include spin chemistry, physics of chemical reactions, ESR and NMR spectroscopy, and molecular ferromagnets.

Both isotope effects sort the isotope nuclei among the reaction products: *CIE selects the nuclei according to their masses,* whereas *MIE selects the nuclei according to their spins and magnetic moments.* This is the first and the most fundamental feature which distinguish MIE and CIE.

The goal of this paper is threefold: (i) to formulate qualitative criteria for discrimination of the two isotope effects; (ii) to compare their scales quantitatively; and (iii) to answer the question whether an upper limit of nuclear spin selectivity exists and how to achieve the highest efficiency of the isotope selection induced by MIE.

II. Radical Pair as a Spin-Selective Microreactor

All events in spin chemistry are mostly associated with the behavior of the radical pair as a spin-selective microreactor responsible for the generation of two types of magnetic effects. The origin of these effects is illustrated by Figure 1. According to the

0009-2665/95/0795-2507$15.50/0

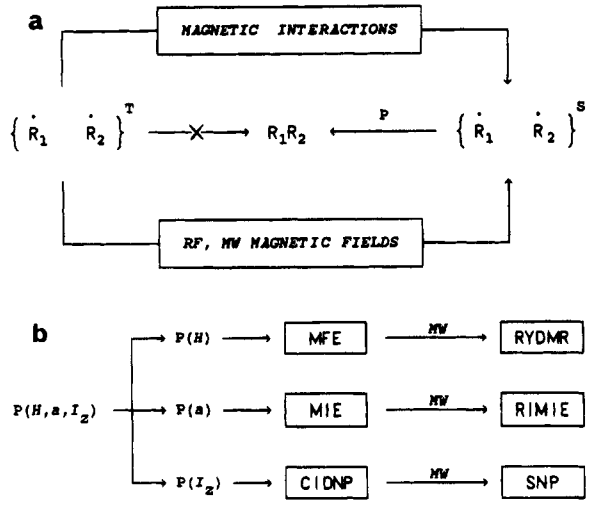

Figure 1. Magnetic interactions and radio frequency or microwave magnetic fields transform the nonreactive triplet radical pair $(R_1^{\bullet}\,{}^{\bullet}R_2)^T$ into the reactive singlet pair $(R_1^{\bullet}\,{}^{\bullet}R_2)^S$ (a). The probability P of the chemical coupling in the pair is a function of magnetic field H, HFI energy a, and nuclear spin orientation I_z (b), resulting in generation of the two types of magnetic effects.

key paradigm of spin chemistry, a radical pair (RP) in triplet spin state cannot transform into the reaction products. In order to react, a triplet–singlet spin conversion is required which is induced either by static magnetic interactions, inherent to RP itself or by radio frequency or microwave irradiation of the RP. The static magnetic interactions result in the dependence of chemical reaction probability P in RP on the magnetic field H, on the HFI energy a, and on the nuclear spin orientation I_z in the RP partners.

Three magnetic effects of the first generation follow from these dependences: MFE, magnetic field effect; MIE, magnetic isotope effect; CIDNP, chemically induced dynamic nuclear polarization. Radio frequency or microwave irradiation induces three new effects of the second generation: RYDMR, reaction yield detected magnetic resonance; RIMIE, radio-induced magnetic isotope effect; SNP, stimulated nuclear polarization. The correspondence between these two sets of effects is demonstrated by Figure 1.[3]

A. The Key Concept of Spin Chemistry

Experimental observation of the magnetic effects definitely proves that the key concept of spin chemistry, namely, spin forbiddenness of chemical reactions, is a fundamental phenomenon. Nevertheless, the question remains how strict this forbiddenness is and how it can be probed quantitatively. Only recently has this problem been solved experimentally by Step *et al.*[4]

In the simplest form the key concept assumes that a caged triplet RP is unable to experience recombination or any other chemical coupling resulting in a molecule (or molecules) in single spin state. To check this statement Step *et al.*[4] have investigated the photoinduced racemization of optically active (*S*)-(+)-α-methyldeoxybenzoin (MDB) which is known to proceed via α-cleavage of C–CO bond and production of triplet RP consisting of benzoyl and *sec*-phenethyl radicals:

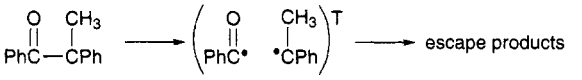

The loss of optical activity is supposed to take place in RP due to fast molecular tumbling of radical partners, so if the recombination of radicals in the triplet RP really occurs, the regenerated ketone molecule is expected to be racemic. Measuring the optical activity of ketone under photolysis as a function of chemical conversion; one can determine the reaction probability P in the RP (see section IV.B).

This approach has been used by Step *et al.* to determine P in the MDB photolysis in benzene at room temperature by monitoring the circular dichroism as a function of conversion.[4] The small value of $P = 0.04$ measured experimentally means that not more than 4% of initially formed triplet RPs recombine to reform the starting ketone. However, it is necessary to take into account that there are two sources of regenerated ketone molecules, i.e., the primary spin-correlated triplet pairs and the radical pairs created by the encounters of freely diffusing radicals which avoid the recombination in the primary triplet pairs. In order to resolve these contributions the photolysis of optically active MDB in benzene has been carried out in the presence of radical scavengers.[4] Under this condition photoracemization was found to be completely suppressed even at a rather small concentration of radical acceptors. This result unambiguously evidences that even a small value of $P = 0.04$ obtained under the photolysis entirely belongs to the contribution of spin uncorrelated RPs created by encounters of randomly diffusing individual radicals. The general conclusion is that the recombination of triplet RP in nonviscous solutions is indeed spin forbidden, so that the equality $P = 0$ is satisfied within the accuracy of 1–2%.

Furthermore, the ^{1}H CIDNP of the starting ketone and other products observed under photolysis of MDB in benzene was shown to be completely suppressed by the addition of radical scavengers,[4] indicating again that there is no geminate cage recombination as well as other cage reactions in the triplet radical pair. This is the *first quantitative proof of the key concept of spin chemistry.*

B. Radical Pair Dynamics

A radical pair is a dynamical system from which the radicals can diffuse apart, traveling randomly in space and time, and then return and reencounter. During these travels there occurs the pair spin conversion which is governed by magnetic interactions in radicals and results either in triplet–singlet transformation of the pair (if its starting state is triplet) or in singlet–triplet transformation (for pairs with the singlet starting state).

To generate a molecule from the triplet RP at least four events should be temporally synchronized.

First, the radicals leaving the RP at the moment $t = 0$ should return and reencounter at a certain moment t. This process which generates successive

contacts of RP partners is described by the molecular or diffusional dynamics.

Second, at the same instant t the pair should necessarily be in the singlet state to be ready to form a molecule. This process is controlled by spin dynamics, i.e., the dynamics of triplet−singlet conversion.

Third, during their diffusion the radicals may undergo chemical transformations (dissociation or scavenging) and yield a new, chemically distinct RP instead of the initial one. However, for a primary molecule to be formed the pair is required to survive the time interval t. The probability of this event is determined by the chemical dynamics.

Fourth, the pair being able to react (i.e., having survived to time t and being at this time in contact and in the singlet state) recombines into a molecule if a favorable orientation of the partners is achieved by rotational dynamics.

Thus, the birth of a molecule is a result of the collective efforts and coordinated choreography of three dynamics—spin, molecular, and chemical, and the evolution of RP along the reaction trajectories on the potential energy surface reflects all these dynamics.

The key act of the magnetic scenario is the spin dynamics governed by the magnetic interactions, among which Zeeman electron and hyperfine interactions are of the first priority, since they are responsible for the magnetic effects in chemical reactions. Magnetic dipolar interaction of electrons and the spin-rotational coupling induce electron spin relaxation which often makes a considerable and sometimes predominant contribution to the spin dynamics, but in these cases magnetic effects turn out to be suppressed. From this point of view, the dipolar and spin-rotational interactions are harmful, provoking the competitive spin interconverison, which should be considered as a leakage in spin evolution controlled by Zeeman and Fermi interactions.

The spin dynamics is modulated by the diffusional molecular dynamics and restricted by the survival time of the RP. Molecular dynamics varies the distance r between the RP partners and, consequently, modulates exchange interaction $J(r)$ which, in turn, influences the rate of spin conversion and, finally, the nuclear spin selectivity. The chemical reaction of the RP partners (addition, decomposition, scavenging, etc.) destroys the pair restricting the time and, therefore, the completeness of triplet−singlet conversion. The goal of the general theory of the RP evolution is to integrate the cooperative effects of these three dynamics and to calculate the probability of chemical coupling in the RP.

There are two levels of the theory which may be classified as nonempirical and semiempirical ones. In terms of the nonempirical theory the molecular and spin dynamics are considered simultaneously, whereas the semiempirical theory ignores their correlation and treats them independently.

Nonempirical theory is based on the numerical solution of a stochastic Liouville equation, which describes both molecular and spin dynamics of the radical pair jointly, taking into account the exchange interaction and spin selective chemical reaction as well. The exchange potential J is assumed to be an exponential function on interradical distance r similar to that for a hydrogen-like molecule:

$$J(r) = J_0 \exp[-\lambda(r - d)] \quad (1)$$

where λ is a characteristic parameter and d is the difference of the closest approach of radicals in the pair.

The nonempirical theory has been developed by Freed, Pedersen, Salikhov, Lawler, Haberkorn, *et al.* and summarized in a monograph;[1a] a comprehensive list of references on the theoretical papers is given in an excellent review by Steiner and Ulrich.[5]

Exchange interaction, $J(r)$, is a short-range potential which rapidly decays at distances of the order of a molecular diameter. In other words, it affects only very short trajectories of diffusional motion of radicals in pair. The time that a pair spends along these trajectories is short, significantly shorter than that of triplet−singlet conversion. Therefore, as a rule, the short diffusion trajectories are inefficient for spin conversion. The prevailing contribution into the triplet−singlet conversion is due to long and continuous trajectories, but along these trajectories exchange interaction between far distant radicals in the pair can be neglected. As a consequence, all three dynamics—spin, molecular, and chemical—can be treated as independent; it is the basis for the semiempirical theory of the integrated spin dynamics.

The probability of molecule generation from a RP in the nuclear spin state ab is determined by the integral

$$P_{ab} = \int_0^\infty \epsilon |C_{S,ab}(t)|^2 f(t) \exp(-kt)\, dt \quad (2)$$

The factor $|C_{S,ab}(t)|^2$ describes spin evolution of the pair, being the probability of finding the pair in singlet state at time t. It can be found by solving the time-dependent Schrodinger equation for electron−nuclear spin functions with spin Hamiltonian which includes Zeeman and Fermi interactions driving the spin evolution. For the particular case of a triplet RP as a precursor

$$|C_{S,ab}(t)|^2 = \sin^2(Q_{ab}t) \quad (3)$$

where Q_{ab} is the triplet−singlet mixing matrix element. For instance, in high magnetic field, when only one component of the triplet spin manifold with zero electron spin projection T_0 is mixed with the singlet spin state

$$Q_{ab} = {}^1/_2[(g_a - g_b)\beta H + \sum_i a_i m_i^a - \sum_i a_i m_i^b] \quad (4)$$

where g_a and g_b are the g-factors of partners a and b in RP, a_i and a_j are the hyperfine coupling constants at nuclei of i and j types, and m_i^a and m_j^b are the projections of the i type of nuclear spins in the a partner and that of the j type of nuclear spins in the b partner, respectively.

Evidently, the spin state of a RP oscillates between singlet and triplet with the characteristic time $t = \pi/Q_{ab}$ which ranges from 10^{-7} to 10^{-10} s, depending on the Q_{ab} value. Certainly, for the RP with $J \neq 0$ the oscillation frequency depends also on the J value.

The term $\exp(-kt)$ in eq 2 accounts for the chemical dynamics of the pair and defines the survival probability of the pair at time t; k is the rate constant for the chemical transformation of RP.

Spin dynamics is superimposed on the molecular dynamics which is described quantitatively by the function $f(t)$, the probability that the radicals having escaped from the pair at $t = 0$ return and reencounter for the first time at instant t. The most favorable diffusional trajectories are those for which the time of the first reencounter coincides with the time of triplet–singlet conversion.

The well-known and frequently used function $f(t)$ has been proposed by Noyes:[6]

$$f(t)_N = mt^{-3/2} \exp(-\pi m^2/p^2 t) \quad (5)$$

where $p = \int_0^\infty f(t)_N \, dt$ is the total probability that the radicals reencounter at least once during the RP lifetime, $(1 - p)$ is then the probability that radicals never return and reencounter. The parameters p and m are approximately

$$p \approx 1 - (^1/_2 - 3\rho/2\sigma)^{-1} \quad (6)$$

$$m \approx 1.036(1 - \rho)^2(\rho/\sigma)^2\nu^{1/2} \quad (7)$$

where ρ is the diameter of contact pair, σ is the distance of the root mean square diffusional displacement of radicals $\sigma^2 = 6D/\nu$, ν is the frequency of the diffusional jumps, and D is the diffusion coefficient.

Molecular dynamics of pairs in liquids has been discussed critically by Razi Naqvi *et al.*[7] They have found the exact expression for the function $f(t)$ different from Noyes' one:

$$f(t)_{RN} = \frac{b}{(\pi Dt)^{1/2}}\left(\frac{d}{r_0}\right)\left\{\exp[-(r_0 - d)^2/4Dt] - B(\pi Dt)^{1/2}\exp[B^2Dt + B(r_0 - d)] \times \operatorname{erfc}\left[B(Dt)^{1/2} + \frac{r_0 - d}{2(Dt)^{1/2}}\right]\right\} \quad (8)$$

where r_0 is the initial distance between the partners in the starting RP, d is the distance of the closest approach of partners in pair, $B = (b/D) + d^{-1}$, $b = \nu l/4$, ν is the frequency of the diffusional jumps, and l is an average free path of a radical.

For two-dimensional molecular dynamics (diffusion in thin films, Langmuir–Blodgett molecular layers, etc.) the $f(t)$ function has been derived and discussed by Deutch.[8] For the molecular dynamics of ion–radical pairs (diffusion in Coulomb potential) various functions $f(t)$ have also been proposed (see, for instance, ref 9). Molecular dynamics in a microreactor of confined geometry (micelles, zeolite or porous glass cavities, etc.) has been treated by Sterna *et al.*[10] and independently by Tarasov and Buchachenko.[11]

The RP recombination probabilities in certain nuclear spin state ab are determined by eq 2. Its solution with the function $f(t)_N$ has been obtained by den Hollander,[12] whereas that for the function $f(t)_{RN}$ has been obtained by Belyakov and Buchachenko.[13] The experimental tests on these solutions will be discussed later in section VI.A.

The total recombination probability in the pair should be found by summation of P_{ab} over all nuclear spin states ab and multiple reencounters. Similarly, the probability of any other reaction in RP can be found; the difference is only in coefficient ϵ which characterizes the branching ratio of specified intrapair reaction channels, i.e. recombination, disproportionation, etc. The detailed analysis of the theory goes beyond the scope of this review and can be found in monographs[1] and review.[5]

C. MIE-Induced Isotope Selection

The MIE was discovered independently by two Russian groups in 1976–1977,[14] although its possibility was mentioned by Lawler and Evans in 1971,[15] but its magnitude was thought to be negligible and hardly detectable. The great contribution to the experimental studies on MIE has been done by the research teams from the Institute of Chemical Physics and Columbia University.

MIE-induced sorting of isotope nuclei can be exemplified by the photolysis of dibenzyl ketone (DBK) which is known to occur via the fragmentation of the DBK molecule excited in triplet state and generation of triplet radical pair (Scheme 1). The triplet radical pair then either undergoes the HFI-induced triplet–singlet conversion and recombines recovering the starting DBK molecule, or dissociates into the separate radicals $PhCH_2$ and $PhCH_2CO$; the latter decomposes into $PhCH_2$ and CO. Dibenzyl $(PhCH_2)_2$ and carbon monoxide are the reaction products in nearly quantitative yields.

The rate of triplet–singlet conversion in the magnetic RPs, i.e. in pairs with magnetic ^{13}C nuclei in phenacyl (or benzyl) radicals, is much higher than that in nonmagnetic pairs containing ^{12}C nuclei. For this reason the former have an advantage in recombining and regenerating DBK molecules, while the delay of triplet–singlet conversion in the latter makes them predominantly dissociative. As a result, the regenerated DBK molecules accumulate ^{13}C nuclei, whereas dibenzyl and carbon monoxide are enriched with ^{12}C nuclei. Thus, due to the difference in the spin conversion rates, RP sorts the nuclei according to their magnetic moments and dispatches the magnetic and nonmagnetic nuclei into the different chemical products (Scheme 1).

This reaction was the first example of the MIE-induced isotope separation.[14a] The second example is the benzoyl peroxide photolysis sensitized by triplet acetophenone (Scheme 2).[14b]

Fermi interaction is significant only in the secondary RP composed of benzoyl and phenyl radicals; therefore, this pair is a spin-selective microreactor. HFI in ^{13}C phenyl radicals accelerates the triplet–singlet conversion and stimulates the recombination of benzoyl and phenyl radicals resulting in phenyl benzoate enriched with ^{13}C. The competition of diffusional separation of radical partners with ^{12}C nuclei favors the impoverishment of other products with ^{13}C isotope.

The thermal decomposition of benzoyl peroxide is known to proceed along the same mechanism but via singlet RPs. Their singlet–triplet conversion is faster for the magnetic pairs with ^{13}C nuclei and, consequently, the magnetic RPs preferentially dis-

Scheme 1. The Isotope Selection in the Dibenzyl Ketone Photolysis

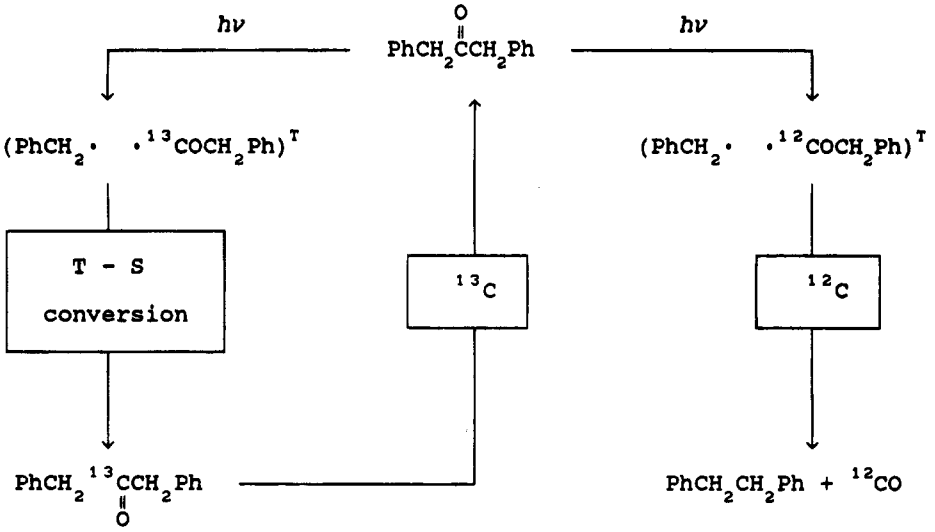

Scheme 2

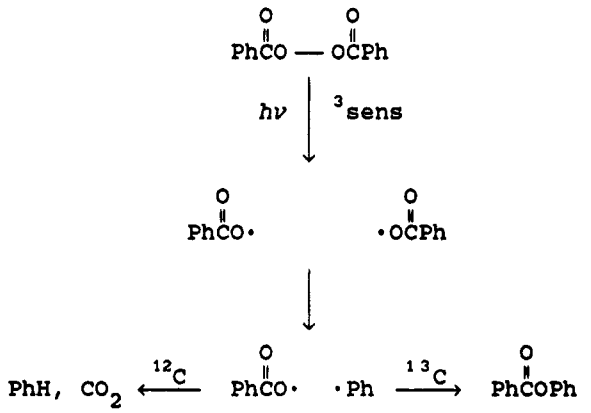

sociate into separated radicals which mostly transform to benzene molecules, whereas nonmagnetic pairs mainly recombine. As a result, benzene molecules generated in thermal reaction accumulate ^{13}C nuclei but phenyl benzoate is enriched with ^{12}C nuclei,[16] exactly in contrast to sensitized photolysis.

MIE is a phenomenon of fundamental importance. Besides the obvious self-interest, it offers a new tool for probing the reaction mechanisms, the kinetics of radical pair reactions, and chemical physics of spin selectivity.[2e] MIE can be responsible for unusual isotopic distribution in geochemical and space materials. At least the hypothesis of chemical MIE-induced fractionation should not be discarded since chemical evolution of matter is a collection of great number of chemical reactions, some of which might be spin selective. They have fractionated magnetic and nonmagnetic nuclei for many millions of years, and now, analyzing the isotope anomalies as an echo of the fractionation, one can try to reconstruct the pathways of chemical evolution and the fate of the substances in nature.

MIE may also operate in biochemical processes so it can be considered as a mechanistic tool in biochemistry. It can arise in spin-selective reactions of carbenes, triplet molecules, ions, and other high-spin chemical species, so that the radical pair is not the only source of MIE.

III. Kinetic Theory of MIE

As a rule, CIE is associated with the energy-expensive steps of chemical processes (bond scission, abstraction reaction, rearrangement, etc.), whereas MIE occurs in energy-cheap elementary processes which require low activation energy if any (such as atom or radical recombination, the addition of atoms or radicals to triplet molecules, etc.). The former belong usually to the rate-limiting stages, the latter are treated as the nonlimiting ones. This is the reason that the kinetic theory of MIE and CIE, as well as kinetic equations describing the isotope selection, are different in many aspects. In this section the comparative analysis of the kinetic theories of MIE and CIE is presented.

A. Irreversible Reactions

For the irreversible chemical transformation of a molecule A (and its isotopomer A*) with the rate constant k (and k^*, respectively) into the product molecules M and N along the channels i and j (Scheme 3) there is no problem in deriving the

Scheme 3

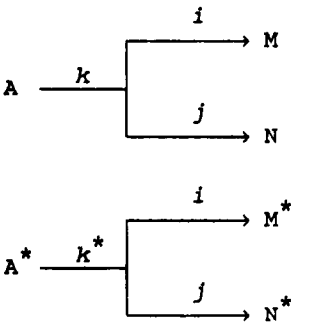

equations for the reaction rates and isotope balance via routine mathematics of simple kinetics. The following parameters are to be determined: $\delta = [A^*]/[A]$ is the content of starred isotope in chemically reacting system; δ_0 is that for the molecule A before reaction; $S = \delta/\delta_0$ is the isotope enrichment:

$$F = ([A]_0 - [A])/[A]_0 = 1 - [A]/[A]_0$$

$$F^* = ([A^*]_0 - [A^*])/[A^*]_0 = 1 - [A^*]/[A^*]_0$$

are the chemical conversions of A and A* molecules, respectively; $\alpha = k^*/k$ is the magnitude of the isotope effect.

In terms of these definitions the time dependence of S obeys the equation

$$S = \exp[-(\alpha - 1)kt] \quad (9)$$

whereas S as a function of chemical conversion can be expressed in two equivalent forms:

$$S = (1 - F)^{\alpha-1} \qquad S = (1 - F^*)^{(\alpha-1)/\alpha} \quad (10)$$

Experimentally detectable values are S, F, or F^*, although usually it is much easier to measure the overall chemical conversion

$$F_{\text{exptl}} = 1 - ([A] + [A^*])/([A]_0 + [A^*]_0)$$

rather than F and F^* separately.

Equation 10 can then be transformed into the following form:

$$S = [(1 - F_{\text{exptl}})[(1 + \delta_0)/(1 + \delta)]]^{\alpha-1} \quad (11)$$

where the experimentally measurable parameters are S, F_{exptl}, δ, and δ_0. In general, the final target is the magnitude of the isotope effect α, i.e. the one-step enrichment coefficient.

For the particular case of primary CIE these equations predict the enrichment of the remaining A with starred isotope if it is larger in mass (then $k^* < k$, $\alpha < 1$, $dS/dt > 0$) or, on the contrary, its impoverishment with starred isotope if it is smaller in mass, since $k^* > k$, $\alpha > 1$, $dS/dt < 0$. By the way, eqs 9–11 are the generalization of the well-known Bernstein's equation for the CIE-induced isotope selectivity.[17]

Similarly, it is rather simple to derive the equations for the time and chemical conversion dependencies of the isotope content in product M (or N) by treating the corresponding channels i and j as isotopically insensitive. They are identical for M and N:

$$\delta_M = \delta_N = [M^*]/[M] = [N^*]/[N] = \delta_0(1 - e^{-k^*t})/(1 - e^{-kt}) = \delta_0[1 - (1 - F)^{\alpha}]/F \quad (12)$$

The above equations describe the isotope selection induced by CIE since the transformation of A into M (or N) is the rate-limiting process and the branching ratio of channels i and j is assumed to be unaltered by isotope replacement. Now let us suppose that the molecule A transforms irreversibly into a radical pair which generates the molecule M via a spin-selective and, therefore, a nuclear spin-selective process, whereas the N molecule is formed in a spin-independent, isotopically nonselective process (Scheme 4).

For the sake of simplicity one can neglect for a while CIE and regard $k^* = k$, i.e., to refer isotope redistribution exclusively to the RP in which only MIE is supposed to operate. It then follows from the kinetic treatment

$$\delta_M = \delta_0(k_1^*/k_1)[(k_1 + k_2)/(k_1^* + k_2)] \quad (13)$$

Scheme 4

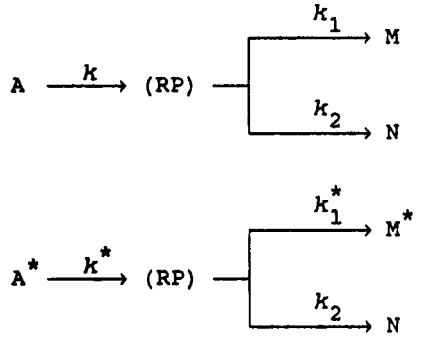

Introducing $\alpha = k_1^*/k_1$ and taking into account that the probabilities of the birth of M and M* molecules in RPs are

$$P = k_1/(k_1 + k_2) \qquad P^* = k_1^*/(k_1^* + k_2) \quad (14)$$

respectively, one obtains

$$\delta_M = \delta_0(P^*/P) = [\delta_0\alpha(k_1 + k_2)/(\alpha k_1 + k_2)] \quad (15)$$

If the spin state of RP is triplet, the probability of intrapair reaction is negligible (see section II.A), i.e. k_1 (and k_1^*) $\ll k_2$, then

$$\delta_M \approx \alpha\delta_0 \quad (16)$$

where α is the MIE magnitude.

For instance, the triplet-sensitized benzoyl peroxide photolysis strictly obeys this kinetic scheme: the RP recombination product phenyl benzoate is not identical to the starting benzoyl peroxide molecule A. The isotope enrichment of phenyl benzoate δ_M measured by Molin *et al.*[14b] follows eq 16. In contrast, for the direct photolysis or thermolysis (via singlet RPs), when both k_1 and k_1^* are comparable with k_2 and cannot be neglected, the more general eq 15 should be used. In the general case, when both isotope effects, classical in the first step ($k^* \neq k$) and magnetic in the second step ($k_1^* \neq k_1$), coexist, it is still not difficult to obtain the equation for the overall isotope enrichment, namely

$$\delta_M^{\text{total}} = \delta_M(\text{CIE})\delta_M(\text{MIE}) \quad (17)$$

where δ_M(CIE) and δ_M(MIE) are determined by eqs 12 and 13, respectively. This means that the total isotope content is a product of the separate contributions of both concomitant isotope effects.

B. Reversible Reactions

The reversibility of the reaction (Scheme 5) implies partial regeneration of the starting molecules from the radical pair. As for Scheme 4, the product N is

Scheme 5

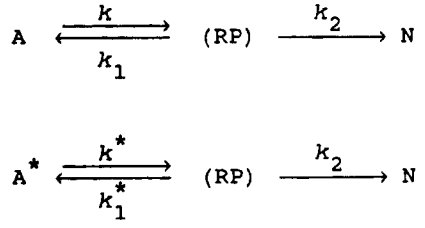

again supposed to be formed in spin-nonselective process (for example, from radicals escaping RP by diffusion). However, in contrast to Scheme 4, the product M is now identical to the starting molecule A which is regenerated in a spin-selective process. This scheme perfectly describes the photolysis of dibenzyl ketone (DBK) in homogeneous solutions (see Scheme 1).[2a]

As above, ignoring for a while CIE in the first step of dissociation of A in RP, i.e. putting $k^* = k$, one can derive the equations for isotope enrichment S of A molecules using the kinetic principles formulated in previous section:

$$S = (1 - F)^{\gamma} \tag{18}$$

$$S = (1 - F^*)^{\gamma^*} \tag{19}$$

$$S = [(1 - F_{\text{exptl}})(1 + \delta_0)/(1 + \delta)]^{\gamma} \tag{20}$$

However, in contrast to eqs 10 and 11 describing the isotope enrichment in irreversible reactions (Schemes 3 and 4), the coefficients γ and γ^* in eqs 18–20 do not only depend on the isotope effect value $\alpha = k_1^*/k_1$ itself, but also on the kinetic parameter k_1/k_2 which characterizes the reaction reversibility, i.e. the regeneration of A:

$$\gamma = \frac{1 - \alpha}{(k_1/k_2)^{-1} + \alpha} \qquad \gamma^* = \frac{1 - \alpha}{(k_1/k_2)^{-1} + 1} \tag{21}$$

Thus, the isotope enrichment in the reversible reactions is strongly dependent on the chemical conversion; the stronger the dependence is the higher the regeneration probability of the starting molecules is. As an illustration, the values of S calculated by eq 18 at the fixed parameters $F = 0.9$ and $\alpha = 1.4$ (quite realistic and attainable at the photolysis of dibenzylketone) are shown below as a function of k_1/k_2 ratio:

k_1/k_2	0.1	0.1	10.0	10^2	10^3
S	1.084	1.469	1.849	1.923	1.928

Such a behavior of S is physically very clear and easily predictable: each regenerated molecule A has a chance to experience the secondary photodissociation in RP and again, after secondary regeneration, to repeat many times the successive dissociation–regeneration cycles. Each regeneration event is spin selective and, therefore, nuclear spin selective. As a result, the overall photolysis looks like a step-by-step multicascade process of isotope selection which collects the isotope nuclei (for instance, ^{13}C in DBK photolysis) in the remainder of starting molecules.

Equations 11–21 describe the isotope enrichment in terms of kinetic rate constants. By introducing the probabilities P and P^* of regeneration of molecules A and A* (see eq 14), it is easy to rewrite the equations for γ and γ^* in terms of these probabilities:

$$\gamma = \frac{P - P^*}{1 - P} \qquad \gamma^* = \frac{P - P^*}{1 - P^*} \tag{22}$$

A more elegant presentation of S as a function of conversion F has been suggested by Tarasov.[18] He started with simple and evident kinetic equations for A:

$$-\text{d[A]}/\text{d}t = k[\text{A}](1 - P)$$

$$-\text{d[A*]}/\text{d}t = k[\text{A*}](1 - P^*) \tag{23}$$

The reduced ratio of the decay rates for A and A* molecules defines a new one-step enrichment coefficient α_G:

$$\left[\frac{\text{d[A]}/\text{d}t}{k[\text{A}]}\right]\left[\frac{\text{d[A*]}/\text{d}t}{k[\text{A*}]}\right]^{-1} = \frac{1 - P}{1 - P^*} = \alpha_G \tag{24}$$

Then eqs 10 and 11 for S transform to

$$S = (1 - F)^{(1-\alpha_G)/\alpha_G} \tag{25}$$

$$S = (1 - F^*)^{(1-\alpha_G)} \tag{26}$$

$$S = [(1 - F_{\text{exptl}})(1 + \delta_0)/(1 + \delta)]^{(1-\alpha_G)/\alpha_G} \tag{27}$$

$$\lg(1 - F) = \alpha_G \lg(1 - F^*) \tag{28}$$

The two systems of eqs 10 and 11 and eqs 25–28 are perfectly compatible, the former describes S as a function of F in terms of kinetic rate constants, the latter does the same in terms of geminate RP reaction probabilities. Which of these systems should be used preferably, depends on the experimentally accessible parameters. The relationships between α_G and γ, γ^* easily follow from the eqs 22 and 24

$$\alpha_G = 1 - \gamma^* \qquad \alpha_G = (1 + \gamma)^{-1} \qquad \alpha_G = \gamma^*/\gamma \tag{29}$$

Finally, if one takes CIE into account by putting $\alpha(\text{CIE}) = k^*/k$ and determining the total one-step enrichment coefficient α_{total} as a ratio of the decay rates for A and A* molecules, the equation follows

$$\alpha_{\text{total}} = \left[\frac{\text{d[A]}/\text{d}t}{k[\text{A}]}\right]\left[\frac{\text{d[A]}/\text{d}t}{k^*[\text{A*}]}\right]^{-1} = \alpha(\text{CIE})\alpha(\text{MIE}) \tag{30}$$

where α(MIE) is identical to α_G. Thus, the total isotope effect is again equal to the product of the separate CIE and MIE contributions.

Now we analyze a more complicated reaction scheme which, in addition to the spin-selective regeneration of starting molecules, involves another competing and also spin selective reaction (Scheme 6).

Scheme 6

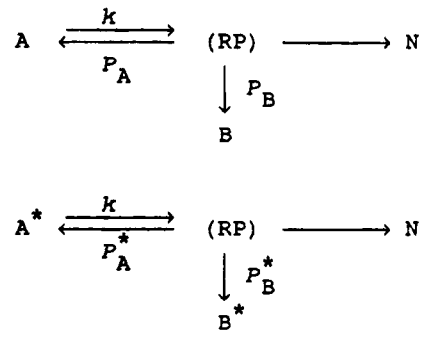

The photolysis of DBK in micelles, in which the addition of $PhCH_2CO$ radical to the para position of $PhCH_2$ ring (head-to-tail recombination of $PhCH_2CO$ and $PhCH_2$ radicals) coexists with the regeneration of DBK molecules (head-to-head recombination), perfectly exemplifies Scheme 6. Spin selective head-to-tail recombination

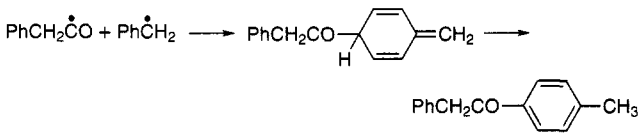

generates *p*-methyl-α-phenylacetophenone (MAP), the product B in Scheme 6.

Another example is the formation of benzaldehyde (product B) in the photolysis of methyldeoxybenzoin as a product of radical disproportionation in RP:

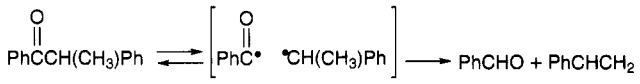

In these cases the distribution of the starred isotope nuclei between the RP cage reaction products A and B is governed by two spin-selective reactions.

Adopting Tarasov's approach, one can derive the equations for the isotope enrichments S_A and S_B for A and B molecules as a function of chemical converison of the starting A molecules. In the approximation ignoring CIE they are as follows:

$$S_A = (1 - F^*)^{1-\alpha_G^A} \qquad S_B = (\alpha_G^A/\alpha_G^B)(F^*/F) \qquad (31)$$

where

$$\alpha_G^A = (1 - P_A)/(1 - P_A^*) \qquad \alpha_G^B = P_B/P_B^* \quad (32)$$

and the important relationship

$$P_A^*/P_A = P_B^*/P_B \qquad (33)$$

between P_A, P_B, P_A^*, and P_B^* implies that the spin dynamics in a common precursor (the radical pair) does not depend on what product molecules, A or B, are generated by the pair. This is a very important and general principle of magnetic equivalence of the reaction trajectories in RPs which has been formulated recently.[19]

The purpose of all the equations derived above is to describe the chemically induced isotope fractionation between the reaction products as a function of chemical conversion according to the following logic: firstly to find the one-step enrichment coefficients α or α_G, and then to evaluate the probabilities P and P^* of intrapair spin selective reactions. Exactly these values are the final targets for two reasons. Firstly, they are amenable to theoretical calculation in the frame of modern theories of integrated spin dynamics and, therefore, give a good occasion to test their validity. Secondly, they allow reliable and accurate prediction of the isotope selection in chemical events and isotope partition between the reaction products.

C. Competition of Radical and Nonradical Reactions

There is a specific and very important class of reactions which include two competing channels, radical and nonradical ones (Scheme 7). By involving

Scheme 7

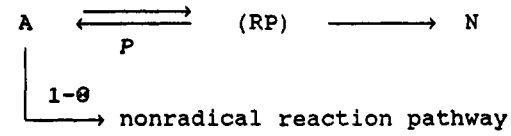

the RP formation and reversible regeneration of the starting molecules A (similar to Scheme 5) the radical pathway is spin selective, whereas being nonradical the concurrent pathway results in the leakage of A reagent (Scheme 7). In terms of the Scheme 7 the total probability of A molecule regeneration is evidently ΘP, where Θ is the radical pathway branching ratio. Analogously, ΘP^* is the regeneration probability for the labeled A* molecules. So, instead of the eq 24 the new equation for α_G now holds:

$$\alpha_G = (1 - \Theta P)/(1 - \Theta P^*) \qquad (34)$$

It allows for the determination of the portion Θ of the radical reaction route by measuring MIE.

To illustrate how strongly Θ affects the α_G values, let us calculate them as a function of Θ for the typical parameters $P = 0.5$ and $P^* = 0.6$:

Θ	1.0	0.8	0.6	0.4	0.0
α_G	1.25	1.15	1.09	1.05	1.00

The competition of the two channels in favor of nonradical pathway (Θ ranges from 1.0 to 0.0) decreases α_G monotonically up to 1.0 and entirely destroys MIE.

An impressive example of a chemical reaction nicely corresponding to Scheme 7 is the triplet-sensitized photolysis of silyl ketone $PhCH_2COSi(CH_3)_2Ph$ in micelles.[20] The direct photolysis of the ketone in heptane, benzene, methanol, and dodecyl sulfate micelles has been shown by CIDNP to occur via singlet RP [$PhCH_2^{\bullet}$ $^{\bullet}COSi(CH_3)_2Ph$], resulting in the products of radical pathway, $PhCH_2Si(CH_3)_2Ph$ and $PhCH_2CH_2Ph$, i.e., under these experimental conditions $\Theta \approx 1$. In contrast, micellar photolysis sensitized by acetophenone is directed along the radical and, therefore, spin selective route only on one third ($\Theta \approx 1/3$), whereas the other two thirds belong to the nonradical channel and include intramolecular insertion reaction resulting in carbene formation:

$$PhCH_2C(O)Si(CH_3)_2Ph \rightarrow PhCH_2\ddot{C}OSi(CH_3)_2Ph$$

whose further transformations yield siloxane products $PhSi(CH_3)_2OH$ and $Ph(CH_3)_2SiOSi(CH_3)_2Ph$. Although the detailed mechanism of this reaction channel is unknown, it was shown to produce neither CIDNP, nor isotope selection.[20-22]

This conclusion derived on the basis of the photochemical product composition is strongly supported by MIE-induced fractionation of ^{13}C and ^{29}Si in silyl

ketone photolysis, which also yields the branching ratio $\Theta \approx {}^1/_3$ (see section VI.C).

IV. Methods for MIE Measurements

As is shown in section III, MIE can be characterized by the ratio of the rate constants k_i^*/k_i of spin-selective reactions, by the ratio of the generation probabilities P^*/P of the molecules from RP, or by the absolute values of k_i^*, P^*, k_i, and P. Now the basic methods of measurements on these MIE parameters will be outlined briefly.

A. Isotope Distribution

Isotope distribution is a MIE fingerprint which should be deciphered to determine the MIE parameters. The principles of the deciphering will be exemplified below.

In the simplest case of a reversible reaction (Scheme 5), if only the isotope composition of the starting reagent is measured, the isotope distribution is shown in section III.B to obey eqs 18–20, from which only the ratio $(1 - P)/(1 - P^*)$, but not the absolute P and P^* values may be estimated. Figure 2 demonstrates the dependence of dibenzyl ketone (DBK) isotope enrichment on the DBK chemical conversion in terms of eq 25.[2a] These dependences are in excellent agreement with the kinetic theory of MIE irrespectively to photolysis conditions (solvent, temperature, viscosity, etc.).

However, it is impossible to extract the absolute values of P and P^* even if the overall isotope composition and the total balance of isotopes in the reaction products are known. Nevertheless, in this case new and unique information on the α_G values for a variety of isotopomers, i.e. for molecular forms with distinct isotopic topology, is available. For instance, for the DBK photolysis in viscous glycerol–*tert*-butyl alcohol mixtures the isotope composition of DBK and dibenzyl (DB) provides the total balance

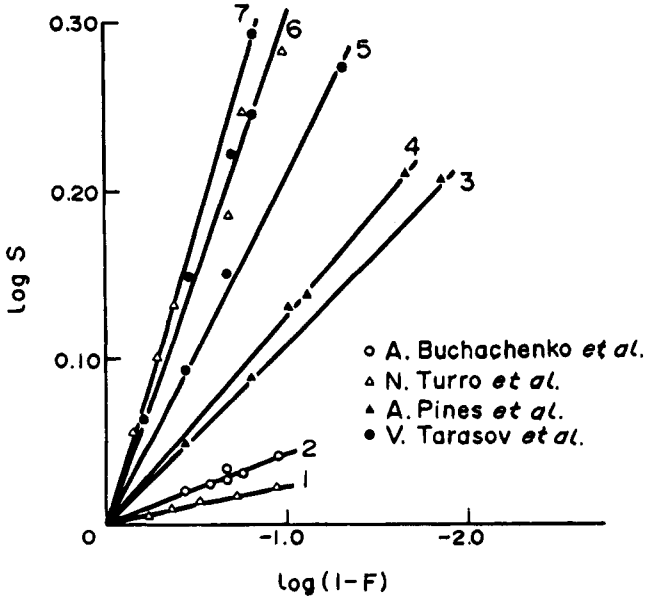

Figure 2. ^{13}C isotope enrichment S as a function of chemical conversion F in terms of eq 25 for dibenzyl ketone photolysis: (1) benzene; (2) hexane; (3) cyclohexanol, 20 °C; (4) cyclohexanol, 0 °C; (5) glycerol, 1700 cp; (6) micelles, HDTCl; (7) glycerol, 2400 cp.

of isotopes which allows, as was shown by Tarasov,[23] the determination of one-step enrichment coefficients α_G for the following isotopic forms of DBK molecules:

$PhCH_2COCH_2Ph$	1
$Ph^{13}CH_2COCH_2Ph$	2
$PhCH_2{}^{13}COCH_2Ph$	3
$Ph^{13}CH_2{}^{13}COCH_2Ph$	4
$Ph^{13}CH_2CO^{13}CH_2Ph$	5
$Ph^{13}CH_2{}^{13}CO^{13}CH_2Ph$	6

It is instructive to inspect this new method in some details. Only the central part of the DBK molecule, $-CH_2COCH_2-$, should be taken into consideration, since in the precursor RP ($PhCH_2^{\bullet}$ $^{\bullet}COCH_2Ph$), HFI is significant and, therefore, strongly influences the RP spin dynamics only for CH_2 and $COCH_2$ groups in the radical partners, while all other HFI couplings can be ignored. For each isotopic modification i of DBK listed above ($i = 1 - 6$) eq 28 acquires the form

$$\alpha_{Gi} = \ln(1 - F_1)/\ln(1 - F_i) \tag{35}$$

where F_1 and F_i are the conversions of the first (isotopically nonlabeled) and ith isotopic forms, respectively. The concentration of any isotopic form can be obtained from the relation

$$C_i = U_i C \tag{36}$$

where C is the total concentration of DBK molecules and coefficients U_i are determined statistically from the isotope distribution:

$$U_1 = (1 - r_1)(1 - r_2)^2 \qquad U_4 = 2(1 - r_1)r_1r_2$$

$$U_2 = 2(1 - r_1)(1 - r_2)r_2 \qquad U_5 = (1 - r_1)r_2^2$$

$$U_3 = r_1(1 - r_2)^2 \qquad U_6 = r_1r_2^2 \tag{37}$$

Here r_1 is the probability for ^{13}C nucleus to be included in the carbonyl group of DBK and r_2 is that for CH_2 group. The measured conversion F_{exptl} evidently follows the equation

$$1 - F_{exptl} = (\sum_{i=1}^{6} C_i)(\sum_{i=1}^{6} C_{i0})^{-1} \tag{38}$$

and conversion F_i of the ith form is described by

$$1 - F_i = C_i/C_{i0} = (U_i/U_{i0})(1 - F_{exptl}) \tag{39}$$

This formula relates the chemical conversion of ith isotopic form of DBK to the total conversion; $U_{i0} = U_i$ at $F_i = 0$.

Since CH_2 groups are transferred from DBK to DB, the ratio of magnetic and nonmagnetic CH_2 groups in DB is

$$(^{13}CH_2)/(^{12}CH_2) = (\sum_{i=2,4,5,6} C_{i0})(\sum_{i=1,3} C_{i0})^{-1} \tag{40}$$

where summation in the numerator runs over the magnetic DB molecules originating from DBK molecules with $^{13}CH_2$ groups ($i = 2,4,5,6$), whereas the summation in the denominator is carried out over the nonmagnetic DB molecules arising from DBK forms with $^{12}CH_2$ groups ($i = 1,3$). Substitution of eqs 39

and 37 for F_i, U_i, and U_{i0} transforms eq 40 into

$$(^{13}CH_2)/(^{12}CH_2) = \frac{r_0 - (1 - F_{exptl})r_2}{(1 - r_0) - (1 - F_{exptl})(1 - r_2)} = \frac{r'_2}{1 - r'_2} \quad (41)$$

where r'_2 is the probability that the CH_2 group in DB contains a ^{13}C nucleus, and r_0 is the initial probability for ^{13}C to occupy any position in DBK molecule ($r_0 = r_1 = r_2$ at $F_{exptl} = 0$). From eq 41 one can derive the isotope balance equation describing the distribution of ^{13}C nuclei in CH_2 groups between DBK and DB:

$$r'_2F_{exptl} + r_2(1 - F_{exptl}) = r_0 \quad (42)$$

The first term represents the fraction of ^{13}C nuclei in DBK CH_2 groups transferred to DB at the conversion F_{exptl} and the second one corresponds to that remaining in DBK CH_2 groups.

The experimental quantity (measurable by mass spectrometry or NMR) is the ratio $^{13}C/^{12}C$. Assuming that the initial distribution of the magnetic nuclei among the DBK or DB molecule is random, the mean probability for the magnetic nucleus to appear at any position in the molecule (see section III) is

$$\langle r \rangle = \delta/(1 + \delta) \quad (43)$$

Then for DB molecule containing 14 carbon atoms isotope balance takes the form

$$14\langle r \rangle_{DB} = 12r_0 + 2r'_2 \quad (44)$$

It is worthy to remember that the reaction changes the isotope contents only for two carbon atoms in DB (namely, those belonging to CH_2 groups), while the isotope composition for the remaining 12 carbons is supposed to be unaltered, since HFI in the radical partners at these atoms has been neglected.

Measuring $\langle r \rangle_{DB}$ and r_0 (the latter can be obtained from isotope content of starting DBK molecules), one can determine r'_2 by eq 44 and, in turn, r_2 by eq 42. For DBK molecules r_1 may be found from the equation similar to eq 44:

$$16\langle r \rangle_{DBK} = 12r_0 + 2r_2 + r_1 \quad (45)$$

For known r_1, r_2, and F_{exptl}, the coefficients U_i and $1 - F_i$ can be obtained from eqs 37 and 39, and, finally, the parameters α_{G_i} may be evaluated (see section VI.A).

The absolute P and P^* values as well as their ratio might be determined only if there is a competition between two spin-selective processes, reversible and irreversible (Scheme 6). Isotope distribution in the products A and B as is shown in section III.B obeys eqs 31 and 32. Particularly, in micellar DBK photolysis these products are the regenerated DBK itself and the *p*-methyl-α-phenylacetophenone (MAP), see section III.B. The isotope contents in these products have been measured[23] and S_B values for MAP as a function of F^* in terms of eq 31 is presented in Figure 3. Experimental data are in excellent agreement with the theory which gives the ratio α_G^A/α_G^B. The α_G^A value is easily determined by eq 25 from the dependence of S_A on F similar to those shown in Figure 2 for DBK.

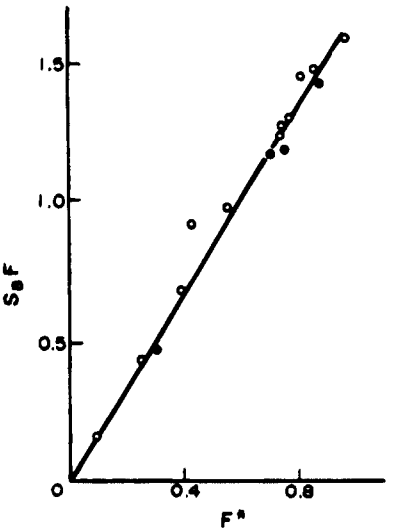

Figure 3. Dependence of isotope enrichment of *p*-methyl-α-phenylacetophenone (head-to-tail recombination product) on the chemical conversion in terms of eq 31. Photolysis of DBK in micelles of hexadecyltrimethylammonium chloride (open circles) and bromide (black circles).

Since DBK and MAP originate from a common precursor, i.e. from the same radical pair

$$P_A^*/P_A = P_B^*/P_B \quad (46)$$

Using this relation and known α_G^A and α_G^B values, one can calculate P_A^* and P_A. For instance, for DBK photolysis in hexadecyltrimethylammonium chloride and bromide micelles, $\alpha_G^A = 1.33$ and $\alpha_G^B = 0.79$, $\alpha_G^A = 1.30$ and $\alpha_G^B = 0.83$, respectively.[23,24] Now P_A and P_A^* can be easily evaluated: $P_A = 0.48$ and $P_A^* = 0.61$ (in chloride micelles), $P_A = 0.52$ and $P_A^* = 0.64$ (in bromide micelles). The MIE magnitude P^*/P is estimated to fall in the 1.23−1.27 range.

A similar approach has been used by Step *et al.*[26] to measure the MIE in the photolysis of methyldeoxybenzoin, $PhCOCH(CH_3)Ph$, which is known to result in the formation of RP [$PhCO^{\bullet}$ $^{\bullet}CH(CH_3)$-Ph] with benzoyl and *sec*-phenethyl radical partners. The two competing spin-selective reactions in RP are the recombination and disproportionation, the former regenerates the starting ketone molecule, the latter results in benzaldehyde and styrene. Measuring isotope compositions S_A and S_B for ketone and benzaldehyde as a function of chemical conversion F according to eqs 31 and 32 the authors[26] have found the ratio of the recombination probabilities P_r^*/P_r as well as that of disproportionation probabilities P_d^*/P_d. Both of these ratios appear to be independent of the magnetic field (in the Earth's field and in a field of 1500 G), a fact which directly evidences that both electron spin-selective reactions in the radical pair are identically selective to ^{13}C nuclear spin. This is an indication of magnetic equivalence of the reaction trajectories in the radical pair.

B. Racemization

An elegant method, specially designed for MIE measurement in optically active compounds, has been developed by Tarasov *et al.*[27] As an illustration one

can consider the photolysis of optically active methyldeoxybenzoin

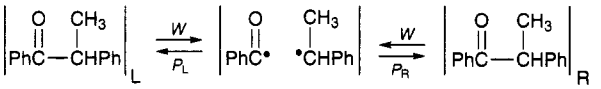

Due to molecular tumbling and inversion of the CH(CH$_3$)Ph radical in RP the initially fixed arrangement of chemical bonds in the vicinity of the optically active center becomes random; therefore, *both* optically active forms of ketone molecule, L and R, can be generated by pair recombination with the probabilities P_L and P_R. Under photolysis by nonpolarized light two equations describe the kinetics of photolysis:

$$d[L]/dt = -w(1 - P_L)[L] + wP_L[R]$$

$$d[R]/dt = -w(1 - P_R)[R] + wP_R[L]$$

where w is the rate of RP generation.

The solution of the equations yields

$$\ln(a/a_0) = \beta \ln(1 - F) \quad (47)$$

where a_0 and a are the optical purity of the ketone before and after photolysis at the chemical conversion F. Equation 47 is similar to that for isotope enrichment (eq 18), since they both describe the competing processes which result in either selection of isotopes or selection of optically active stereoisomers. The coefficient β in eq 47 is

$$\beta = 2P_R/(1 - P_R - P_L) \quad (48)$$

However, since the radical reorientation rate exceeds considerably both the RP decay rate and the RP spin evolution rate, an overall randomization occurs and, therefore, the total recombination probability is $P_r = P_R + P_L$ where $P_R = P_L$. Then, it follows from eq 48

$$P_r = \beta/(1 + \beta) \quad (49)$$

where β can be deduced experimentally by chemical analysis of R and L ketones, or by monitoring circular dichroism as a function of ketone conversion. These considerations and, in particular, the important equality $P_R = P_L$, which implies the magnetic equivalence of the reaction trajectories for R and L recombination in the common RP precursor, has been reliably confirmed experimentally.[27]

Knowing P_r, one can easily evaluate the probability P_d of another competing reaction (disproportionation), measuring the yield χ of its product, benzaldehyde:

$$P_d = \chi/(1 - P_r) \quad (50)$$

This equation evidently follows from the balance of the reactions in RP.

Figure 4 demonstrates the P_r and P_d values determined from the photoinduced racemization of methyldeoxybenzoin as a function of the magnetic field.[27] The relationship between P_r and P_d is shown in Figure 5 which emphasizes that the ratio $P_r/P_d = 6.6 \pm 0.6$ does not depend on the magnetic field up to 15 kG, strongly supporting an idea that the reaction trajectories for the head-to-head RP reaction, R and L recombinations and disproportionation, are magnetically equivalent.[19]

Similar but more complicated equations for the decay of optical activity have been derived for the

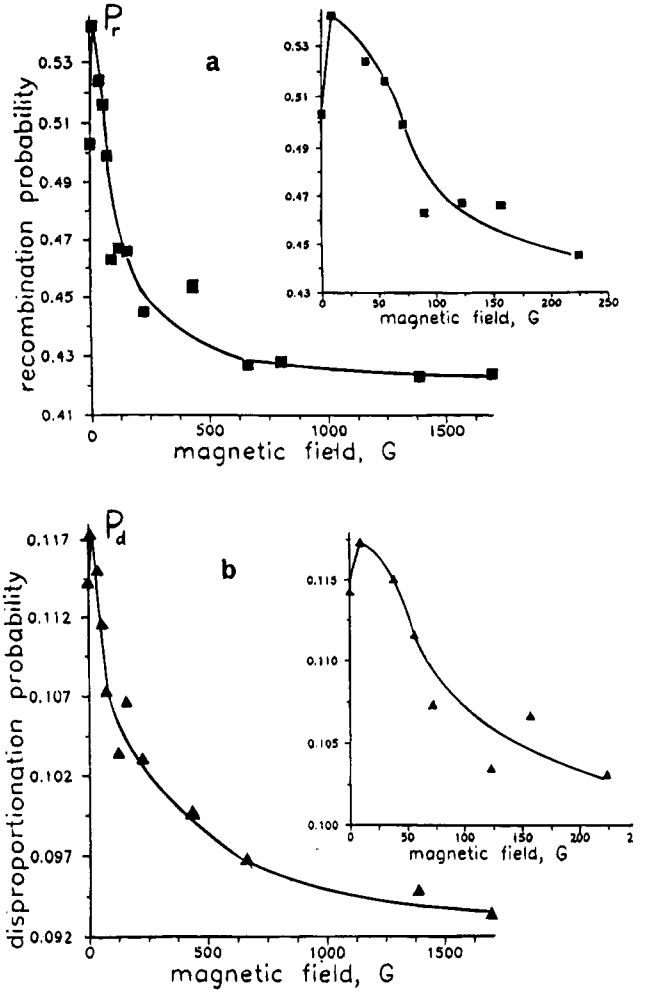

Figure 4. Magnetic field dependences of the recombination (a) and disproportionation (b) probabilities of the radical pairs generated by photolysis of methyldeoxybenzoin in SDS micelles.[27]

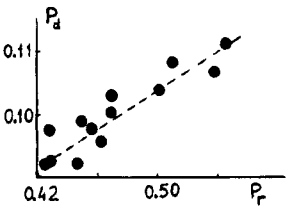

Figure 5. Linear relationship between the recombination P_r and disproportionation P_d probabilities; $P_r/P_d = 6.6 \pm 0.2$ and does not depend on the magnetic field in contrast to the individual P_r and P_d values (cf. Figure 4).

case when the reacting molecule has two optically active centers and the recombination probabilities P_r^* and P_r, as well as their magnetic field dependences, have been measured for two stereoisomers of optically active 2,4-diphenylpentan-3-one[28]

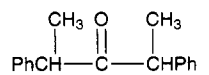

^{13}C labeled and unlabeled at the carbonyl atom (see section VI.A).

C. Direct Kinetic Methods

The dynamics of intrapair reactions can be monitored directly by time-resolved laser-transient absorption or laser-induced fluorescence spectroscopy.

These kinetic methods allow the determination of the rates or rate constants and provide direct information on the reaction probabilities, see eqs 24 and 30. Many excellent examples of applications of these perfect and beautiful methods for measuring MIE which require highly isotropically enriched starting materials have been given by Turro.[2b]

V. MIE versus CIE: Quality

The efficiency of nuclear spin selection is governed by the HFI: the higher the HFI energy, the stronger the nuclear spin system "violates" the electron spin selection rules and differentiates the rates of triplet–singlet conversion in magnetic and nonmagnetic RPs. The HFI dependence is the second feature of MIE, which, in contrast to CIE, may result in measurable isotope enrichment of atoms remote from the reaction center. The reason is that the spin density distribution along the chemical bonds in radicals is attenuated irregularly and may result in high HFI energy at distant atoms. At least it decreases much slower than the perturbation in molecular vibrations induced by isotope replacement. From this viewpoint MIE can be considered as a long-range effect in contrast to the short-range CIE.

The priority in the chemical reaction scenario written by magnetic interactions belongs to spin dynamics which regulates the rate of spin conversion and is strongly influenced by the magnetic field and *g*-factor difference of the RP partners. A high magnetic field sensitivity of the spin-selective reaction kinetics and, consequently, of MIE parameters is the third symptom inherent to MIE only.

As shown in section II the triplet–singlet spin conversion is a result of the joint and coordinated efforts of spin, molecular, and chemical dynamics. Therefore, MIE is strongly affected by the molecular diffusion, translational and rotational motions, and the lifetime of radicals. These MIE properties have nothing to do with CIE characteristics and constitute the fourth important criterion for the MIE/CIE discrimination.

The fifth criterion is the character of temperature dependence: CIE is well known to depend only slightly on the temperature according to Arrhenius equation with the exponential equal to zero-point vibrational energy difference of the isotopically different molecules and the corresponding transition states (we exclude the specific case of tunneling), while the MIE temperature dependence is much more complicated and nonregular involving the temperature dependences of the radical lifetimes, diffusion coefficients, rotational correlation times, and other parameters of molecular and chemical dynamics.

The sign of CIE is unambiguously dictated by the mass ratio of isotopes, whereas the MIE sign depends on the spin multiplicity of the pair of radicals or other chemical spin carriers. More rigorously, it depends on the direction of the spin conversion (from triplet to singlet or vice versa), so the inversion of the spin multiplicity is followed by the inversion of the MIE sign. For example, magnetic isotope effects in triplet-sensitized photolysis and in thermal decomposition of benzoyl peroxide are of opposite signs.[14c,16] The photoreaction includes triplet RP and triplet–singlet spin conversion, while the thermal reaction starts in singlet RP and involves its singlet–triplet conversion (section II.C). In fact, these two chemically identical reactions produce different MIE-induced isotope distributions: in the first case the cage product (phenyl benzoate) is enriched with ^{13}C, whereas in the second case it is enriched with ^{12}C nuclei. Such a dependence of MIE sign on the spin evolution direction is an excellent test for identification of the spin multiplicity of the reactive intermediates and, therefore, for the reaction mechanism elucidation. Scheme 8 provides a summary of the specific and contrasting features of both effects.

Scheme 8. MIE versus CIE: Quality

Symptoms	MIE	CIE
Selectivity parameter	nuclear spin and magnetic moment	nuclear mass
Fermi interaction	dependent	independent
Magnetic field	strong influence	no influence
Molecular dynamics	strong dependence	no influence
Chemical dynamics and radical lifetime	dependent	independent
Temperature effect	strong	weak
Spin multiplicity	strong dependence both in sign and magnitude	no influence

VI. MIE versus CIE: Quantity

A. $^{13}C/^{12}C$ Dyad

Figure 2 demonstrates the feasibility of eq 25 for the quantitative description of the MIE-induced isotope selectivity in DBK photolysis. Both Figure 2 and Table 1 reveal the high sensitivity of the α_G values to the molecular environment which points out their MIE origin. The general trend is that the larger the solution viscosity is, the higher isotope selection is. However, the best selectivity as a rule is attained in microreactors of confined geometry (micelles, zeolite or porous glass cavities, very viscous solutions with spatially restricted diffusion, etc.). Here and further we appeal to α_G omitting the index G.

The α values for the photolysis of some other ketones exhibit a similar trend (Table 1). The typical magnetic field dependences of α for DBK and 2,4-diphenylpentane-3-one (DPP) photolysis depicted in Figure 6 unambiguously demonstrate the dominant contribution of MIE to isotope separation. However, the limiting α at $H \rightarrow \infty$ corresponds to the α(CIE) and CIE-induced isotope selection.

The lowest α have been found to be 1.039, 1.031, 1.020 (see Table 1), 1.041 (DBK photolysis in hexane in magnetic field 500 G[14a]), 1.030 (DBK, 100 kG[29]), 1.043 (DPP, micelles, the lowest limit[28]), so that the value $\alpha = 1.030 \pm 0.010$ can be reliably attributed to the CIE limit which is very close to the square root of ^{13}C and ^{12}C nuclear mass ratio.

The α coefficients have been measured for the different isotope forms of the DBK molecules by the method developed by Tarasov *et al.*[23] and described in section IV.A. The recovered and, therefore, ^{13}C-enriched DBK molecules are formed from RPs with $PhCH_2CO$ and $PhCH_2$ partners in which HFI energies range from 3.8×10^8 to 21.1×10^8 rad/s. (For the extreme cases of RPs arising from ketones 1 and 6, respectively, see section IV.A.)

The α for these ketones as a function of the total HFI energy in the RP precursors of the recovered DBK molecules are presented in Figure 7. The high sensitivity of α to the magnetic HFI energy as well as to the magnetic field (Figure 6) evidences the great predominance of MIE over CIE. By the way, the largest known up to date α value for $^{13}C/^{12}C$ isotope effect found by Turro in the photolysis of phenyl adamantyl ketone (see Table 1) is completely related due to the highest HFI energy in the pair of PhCO and adamanthyl radicals (HFI coupling constants $a(^{13}C)$ are equal to 125 and 132 G, respectively).

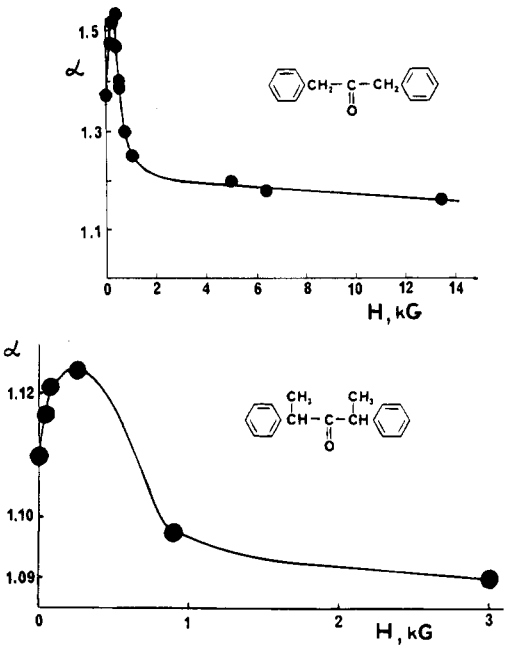

Figure 6. One-step enrichment coefficients α as a function of magnetic field for the photolysis of dibenzyl ketone and 2,4-diphenylpentan-3-one.

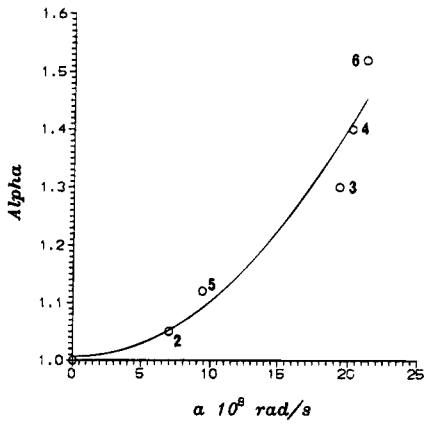

Figure 7. Dependence of the one-step enrichment coefficients α on the HFI energy *a* in the radical pairs (dibenzyl ketone photolysis in hexadecyltrimethylammonium bromide). The numbers refer to the isotopic forms of DBK molecules (section IV.A).

Table 1. ^{13}C One-Step Enrichment Coefficients α for Ketone Photolysis

ketone	α	photolysis conditions	ref
DBK[a]	1.054	hexane, 20 °C, 0.3 cp	Buchachenko *et al.*[14a]
DBK	1.039	toluene, 20 °C, 0.6 cp	Pines *et al.*[10]
DBK	1.031	benzene, 20 °C, 0.65 cp	Turro *et al.*[24c]
DBK	1.062	3-pentanol, 23 °C, 7 cp	Pines *et al.*[10]
DBK	1.095	cyclohexanol, 23 °C, 7 cp	Pines *et al.*[10]
DBK	1.113	cyclohexanol, 0 °C, glass	Pines *et al.*[10]
$PhCH_2{}^{13}COCH_2Ph$	1.37	micelles, HDTCl	Turro *et al.*[29]
$Ph{}^{13}CH_2CO{}^{13}CH_2Ph$	1.20	micelles, HDTCl	Turro *et al.*[29]
$PhCD_2{}^{13}COCD_2Ph$	1.35	micelles, HDTCl	Turro *et al.*[29]
DBK	1.50	glycerol, 2400 cp	Tarasov *et al.*[30]
DBK	1.39	micelles, HDTBr	Tarasov *et al.*[30]
DBK	1.41	micelles, HDBr + NaCl	Tarasov *et al.*[30]
$PhCOCH_2Ph$	1.30	micelles, HDTCl	Turro *et al.*[31]
PhCO adamantyl	1.02	cyclohexane, 20 °C	Turro *et al.*[31]
PhCO adamantyl	1.63	micelles, HDTCl	Turro *et al.*[31]

[a] Dibenzyl ketone.

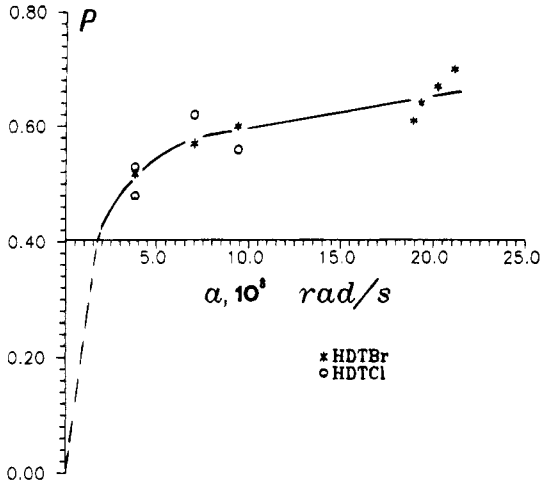

Figure 8. Recombination probabilities of the radical pairs generated by photolysis of DBK in hexadecyltetramethylammonium chloride and bromide micelles as a function of HFI energy in RPs.

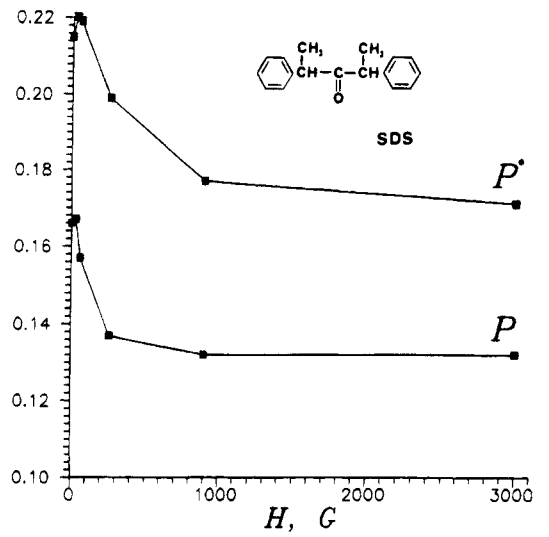

Figure 9. Recombination probabilities P^* and P for the magnetic and nonmagnetic radical pairs generated by DPP photolysis in sodium dodecyl sulfate micelles as a function of magnetic field.

The recombination probabilities for the photogenerated triplet RPs of DBK in micelles as well as for the triplet RPs of *d,l*-2,4-diphenylpentan-3-one (DPP) in micelles have been measured by the methods described in section IV.B. The former are shown in Figure 8 as a function of HFI energy in the pairs of various isotope composition;[2a] the latter are depicted in Figure 9 as a function of the magnetic field.

The dependences $\alpha(H)$, $\alpha(a)$, as well as $P(H)$, $P^*(H)$, and $P(a)$ demonstrate the sensitivity of MIE to the magnetic interactions, to Zeeman and Fermi energy. Figure 10 characterizes the influence of molecular dynamics on the MIE and MIE-induced isotope separation.[23] For the different isotopic forms of DBK molecules there exists an optimal value of diffusion coefficient D, almost identical for all isotopomers, at which α reaches its maximum value and isotope selection is the most efficient. Such a behavior of α is caused by the favorable interplay of spin and molecular dynamics (section II.B) and is similar to that observed for the ^{17}O MIE in the polymer oxidation processes (*vide infra*, next section).

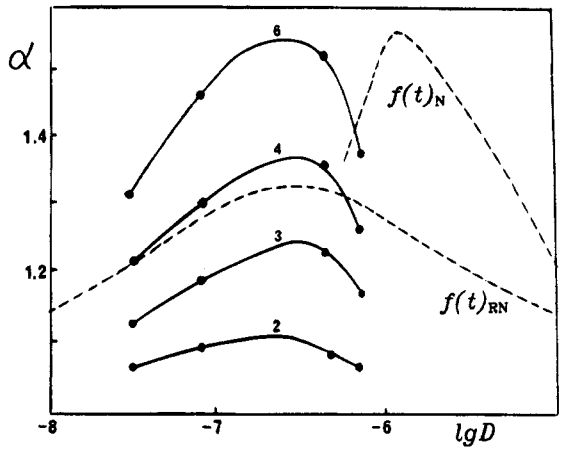

Figure 10. Dependence of α for the photolysis of DBK molecules in glycerol–*tert*-butyl alcohol mixtures on the diffusion coefficients. The numbers on the curves correspond to the DBK isotopic forms (see section IV.A and Figure 7). The diffusion coefficients refer to the TEMPO nitroxide radical whose size is almost identical to that of the partners in the radical pair. The dotted curves are theoretical dependences calculated with Noyes function $f(t)_N$ and Razi Naqvi function $f(t)_{RN}$.

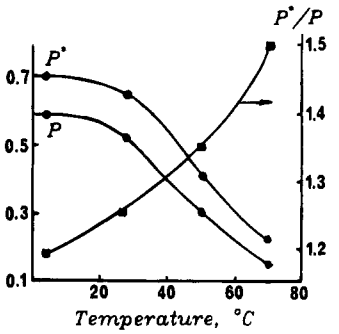

Figure 11. Temperature dependence of the recombination probabilities P^* and P of the magnetic and nonmagnetic RP generated by DBK photolysis. Also shown is their ratio P^*/P as a function of temperature.

For the particular case of DBK photolysis in viscous glycerol–*tert*-butyl alcohol mixtures α has been calculated in terms of two molecular dynamic functions, the Noyes function $f(t)_N$ and Razi Naqvi function $f(t)_{RN}$ (see section II.B). Rather good agreement with experimental results both in position of maximum and the absolute α values has been achieved only with $f(t)_{RN}$ function.[32] The Noyes function certainly fails to give a quantitative description of experimentally observed α(lg D) dependence. This fact seems quite natural because Noyes flight model is hardly adequate to describe the molecular motion in very viscous media.

The temperature dependence of isotope composition of DBK and *p*-methyl-α-phenylacetophenone (MAP) for DBK photolysis in hexadecyltrimethylammonium chloride micelles has been studied by Turro *et al.*[33] Their data recalculated in terms of eqs 31–33 are shown in Figure 11. The absolute values of the recombination probabilities P and P^* were found to decrease differently in the temperature range 0–70 °C: P decreases faster than P^*. As a result the ratio P/P^* increases as the temperature grows (Figure 11).

Such a temperature behavior of MIE is a result of interplay of spin and chemical dynamics. At high

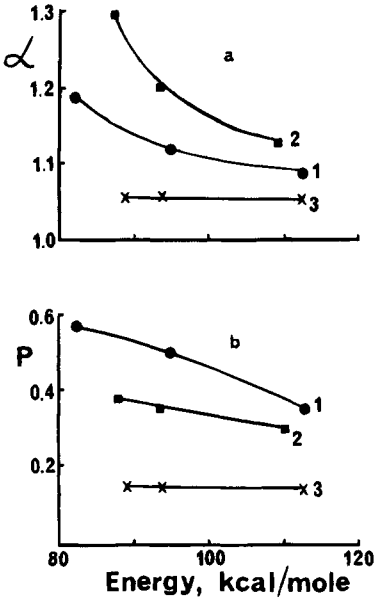

Figure 12. Coefficients α (a) and recombination probabilities P (b) as a function of the light energy in the photolysis of methyldeoxybenzoin (1), dibenzyl ketone (2), and diphenylpentanone (3).[35]

temperatures the rate of $PhCH_2CO$ decarbonylation increases, the lifetime of the radical pair decreases, and the regeneration of DBK molecules drops. However, the MIE value itself increases and partly compensates the reduction of regeneration since for long-lived RP ($\tau_{RP} \gg |Q_{ab}|^{-1}$) the effective rate of triplet–singlet conversion is proportional to $|Q_{ab}|^{1/2}$, whereas for short-lived RP ($\tau_{RP} \ll |Q_{ab}|^{-1}$) it is proportional to $|Q_{ab}|^2$.[34]

Nevertheless, the effect of regeneration depression dominates, it prevails over the increasing MIE itself and, finally, reduces α values from 1.4 at 3 °C to 1.1 at 70 °C.

Such a temperature behavior of P and α indicates the importance of chemical dynamics which restricts in time the RP spin evolution. An even more impressive conclusion follows from the comparison of P values for DBK and DPP photolysis (Figures 8 and 9): the former are three or even four times higher than the latter. The values of P are in accordance with the lifetimes of acyl radicals: elimination of carbon monoxide limits the lifetime of $PhCH_2CO$ radical to 150 ns and that of $PhCH(CH_3)CO$ radical to 22 ns. It means that the triplet–singlet conversion of the RP generated from DPP is more strongly time limited than that of RP from DBK.

Step *et al.*[35] have studied the wavelength effects on the stereoisomerization and $^{13}C/^{12}C$ isotope separation under the photolysis of three ketones, methyldeoxybenzoin (MDB), dibenzyl ketone (DBK), and 2,4-dimethylpentanone (DPP) in SDS micelles. By monitoring the circular dichroism for MDB and DPP and by measuring isotope distribution for all ketones, α and RP recombination probabilities P have been evaluated. Their dependences on the energy of the exciting light are shown in Figure 12. The magnitudes of both P and α for the MDB photolysis and the magnitude of α for the DBK photolysis decrease as the energy of the light quanta increases. However, for DPP no wavelength dependence has been found for both α and P.

At first sight the postulate of hot radicals seemingly explains this intriguing behavior of α and P: the energy excess is expected to be localized on the vibrational modes of acyl radicals and stimulates their decarbonylation, reducing the lifetime and decreasing P and α, similar to the temperature growth. (See Figure 11.) However, this idea is easily discarded by the following arguments. The lifetime of acyl radical PhCO from MDB with respect to decarbonylation is known to be very large, whereas the lifetimes of $PhCH_2CO$ from DBK and $PhCH(CH_3)CO$ from DPP are 150 and 22 ns, respectively. In order to manifest itself in the decarbonylation, vibrational excitations should survive for a time at least ≥ 22 ns. However, the lifetime of vibrational excitation in liquids is known to be only 1–2 ps.

The possibility of local matrix heating induced by vibrational energy energy dissipation should be also rejected on the basis of thermal conductivity measurements[36] which show that thermal equilibrium in organic media for separation 10–15 Å is attained generally in a time shorter than 100 ps. Another argument is again the absence of the wavelength effect on P and α for DPP photolysis.

The wavelength effects have been explained in terms of the competition of adiabatic and diabatic chemical bond dissociation trajectories on the potential energy surface. For MDB and DBK the triplet excited molecules follow $^3\pi,\pi^*-^3\sigma,\pi$ adiabatic trajectories, which produce excited linear acyl radicals at higher energy excitation to a greater extent than at lower energy. The release of the excess energy through enhanced chemical reactivity of linear acyl radical with respect to decarbonylation provides shortening of the lifetime of the primary RP and decreasing of P and α. The absence of the wavelength effect for DPP photolysis indicates that the dissociation of this ketone follows fast and, therefore, diabatic trajectories from $^3\pi,\pi^*$ states to $^3\sigma,\sigma^*$; the latter correlates in orbital symmetry to the ground state of ketone.

Being rather logical and self-consistent this explanation still leaves the two most difficult questions unanswered. The first is why the energy excess in MDB and DBK directs the bond cleavage along the adiabatic trajectories although the opposite proportion and opposite trend should be expected. The second is why the excited DPP preferably chooses the diabatic trajectory rather than the adiabatic one, in contrast to MDB and DBK.

Recently, Tarasov, Turro, and Buchachenko have initiated a new series of experiments aimed at probing the interradical exchange potential in RP through the influence of micelle size on the α and P values.[37] The first results unequivocally demonstrate that only the introduction of distance-dependent electron spin exchange, which retards the rate of HFI-induced spin conversion, allows one to fit theory to experiment quantitatively. They seem promising for clarifying many important details of relations between spin and molecular dynamics.

B. $^{16}O/^{17}O/^{18}O$ Triad

The ^{17}O MIE was mentioned for the first time in 1978[38a] and studied later in the chain processes of polymer and hydrocarbon oxidation by molecular

oxygen,[38b,c] as well as in the endoperoxide thermolysis.[38d]

The chain oxidation of organic compounds occurs via repetitive sequence of two kinetic chain propagation reactions:

$$\dot{R} + O_2 \rightarrow R\dot{O}_2$$

and

$$R\dot{O}_2 + RH \rightarrow ROOH + \dot{R}$$

Here RH is the organic substrate, and $\dot{R}$ and $R\dot{O}_2$ are alkyl and peroxy radicals. The chain termination reaction includes the recombination of peroxy radicals which is expected to be spin selective and, therefore, an isotope-sorting reaction:

$$R\dot{O}_2 + R\dot{O}_2 \rightleftarrows (R\dot{O}_2\ \dot{O}_2R) \rightleftarrows RO_4R \rightarrow R\dot{O} + \dot{O}_3R \rightarrow 2R\dot{O} + O_2$$

The encounter pair of freely diffusing peroxy radicals either recombines resulting in an unstable tetraoxide RO_4R, which decomposes regenerating an oxygen molecule from the central oxygen atoms, or dissociates regenerating peroxy radicals. In the encounter RP the ratio of singlet and triplet spin state populations is 1:3, but being negligibly small in singlet pair, MIE arises almost completely from the triplet–singlet conversion of triplet RP. Due to the magnetic isotope effect, which causes a difference in the rates of spin conversion, the recombination probability of peroxy radicals with terminal ^{17}O atoms is higher than that of radicals with terminal ^{16}O or ^{18}O atoms. As a result, the tetraoxide and, consequently, the recovered oxygen should be enriched with magnetic isotope ^{17}O, while the hydroperoxide molecules should be impoverished.

This spin-selective process is kinetically identical to the DBK photolysis: the molecular oxygen as a reagent is consumed in a partly reversible process but its remainder is enriched with regenerated and, therefore, ^{17}O-rich oxygen molecules, so that the ^{17}O enrichment as a function of oxygen chemical conversion should follow eq 25. Indeed, for the chain oxidation of polypropylene, polyethylene, poly-4-methylpentene, natural rubber, polyisobutylene, and some other polymers in viscous–elastic state the experimentally measured S values as a function of chemical conversion have been found in excellent agreement with this equation.

Figure 13 exemplifies this agreement for the particular case of polypropylene.[38b] The one-step enrichment coefficient $\alpha(^{17}O) = 1.060 \pm 0.010$ is much higher than that for the nonmagnetic nucleus ^{18}O [$\alpha(^{18}O) = 1.015 \pm 0.005$] certifying again that α(MIE) $\gg \alpha$(CIE).

Figure 14 demonstrates the impressive distinction in the temperature behavior of α: for the CIE-induced ^{18}O enrichment the α values reveal only a small decrease as the temperature increases, while for the MIE-induced ^{17}O enrichment the temperature effect is much higher and passes over a maximum

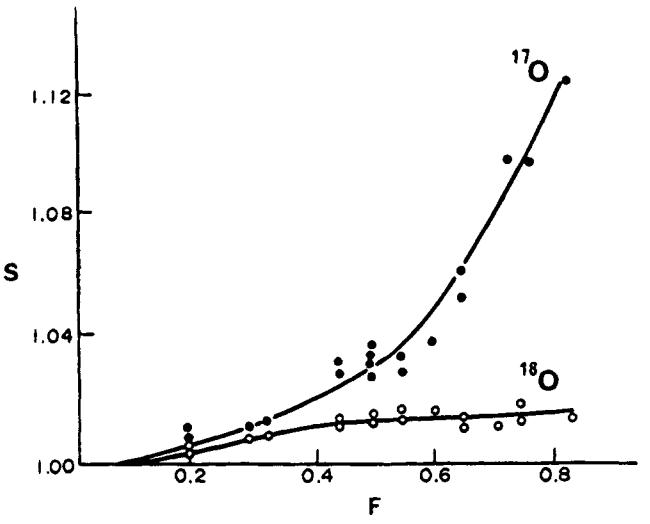

Figure 13. Oxygen isotope enrichment S as a function of oxygen conversion in the polypropylene chain oxidation. The theoretical curve corresponds to $\alpha(^{17}O) = 1.060$.

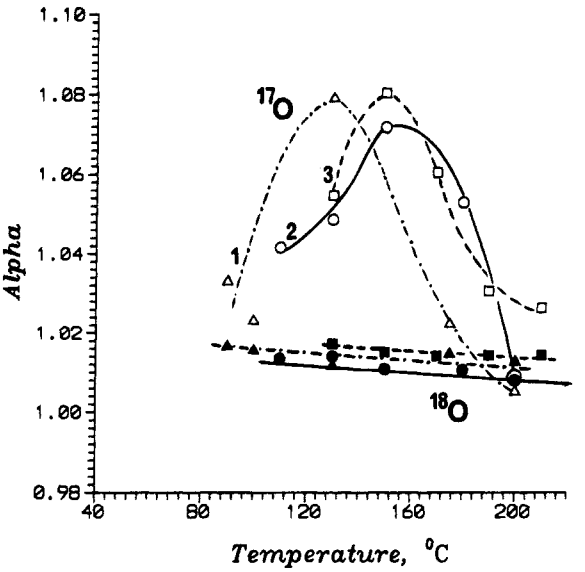

Figure 14. Temperature dependence of the one-step enrichment coefficients α for ^{17}O and ^{18}O in oxidation of polyethylene (1), polypropylene (2), and poly-4-methylpentene (3). The open circles, squares, and triangles correspond to ^{17}O; the filled ones, to ^{18}O.

which reflects the most favorable isotope selection condition when the time scale of molecular dynamics is compatible with that of spin dynamics. The proximity of the diffusional lifetime of the peroxy radical pair and the time of its triplet–singlet conversion provides the best nuclear spin selection in the pair: at higher temperatures the lifetime of RP becomes shorter (fast diffusion) and RP does not have enough time to experience the spin conversion and produce the isotope sorting, whereas at lower temperatures the time of RP survival is longer than that of spin conversion, so that MIE-induced nuclear spin selection is scrambled during the RP lifetime and isotope sorting is ineffective again.

The α values for both ^{17}O and ^{18}O isotopes have been experimentally found to fall as the reaction chain length decreases (Figure 15). This is the evidence that both effects—MIE for ^{17}O and CIE for ^{18}O—originate from the termination reaction shown above. Namely, MIE arises from spin-selective recombination of peroxy radicals into the tetraoxide,

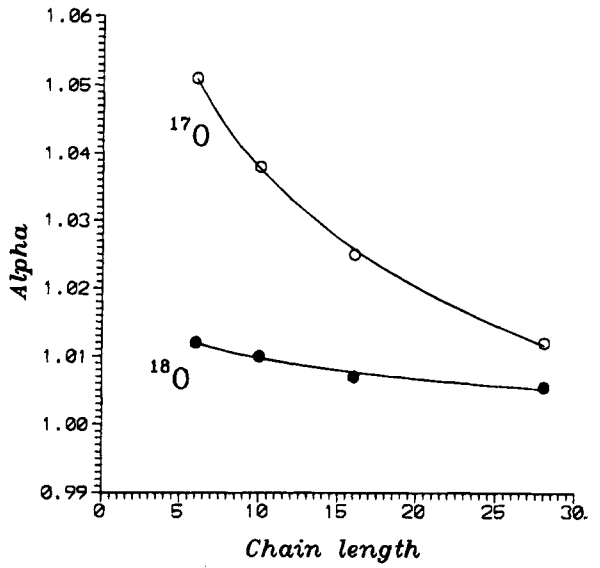

Figure 15. One-step oxygen isotope enrichment coefficients α as a function of the chain length in polyethylene oxidation induced by γ-radiolysis.[38b]

whereas the CIE occurs in the decomposition of tetraoxide according to the following scheme:

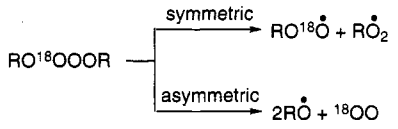

Only the asymmetric oxygen−oxygen bond scission regenerates ^{18}O-enriched oxygen molecules, while the symmetric scission restores the peroxy radicals. Therefore, the number of nuclear spin-selective steps depends on the chain length similarly for both ^{18}O and ^{17}O: it decreases as the chain length increases, in accordance with experimental findings (Figure 15).

In contrast to the oxidation of polymers in the viscous−elastic state, the liquid-phase oxidation of hydrocarbons or polymer solutions leads to the impoverishment of molecular oxygen with ^{17}O and enrichment with ^{18}O.[38c] The opposite signs of isotope effects certainly discount termination reaction as a main source of isotope selection. It has been concluded that another spin-selective reaction

$$\dot{R} + O_2 \overset{k_a}{\rightleftharpoons} (\dot{R}\ O_2) \rightarrow RO_2$$

plays a dominant role in the nuclear sorting. The reaction precursor is the ($R^{\bullet}$ O_2) pair in doublet or quartet spin state, so that the reaction product, doublet spin state peroxy radical, originates only from the former. The reaction from quartet RPs is spin forbidden; therefore, only quartet−doublet spin conversion of these pairs ensures their reaction. Due to HFI, oxygen molecules with ^{17}O react faster than those with ^{16}O or ^{18}O nuclei leading to the MIE and MIE-induced impoverishment of the remaining molecular oxygen with ^{17}O. In contrast, oxygen molecules with ^{18}O react slower than those with ^{16}O resulting in the CIE-induced enrichment of the molecular oxygen with ^{18}O. This concept is supported by the fact that the isotope enrichment does not depend on the chain length of liquid phase oxidation[38c] in contrast to the polymer oxidation. It seems that the magnetic field effect would be informative for discriminating between these two spin selective reactions.

The one-step enrichment coefficients in the liquid-phase oxidation of ethylbenzene, isopropylbenzene, and polypropylene solutions are 1.008 ± 0.003 [α(^{18}O) for CIE] and 0.992 ± 0.002 [α(^{17}O) for MIE]. These values again demonstrate the predominance of MIE over CIE: the negative MIE for ^{17}O compensates the positive CIE for ^{17}O and even exceeds it by magnitude.[38c]

The difference in ^{17}O isotope behavior in two processes—liquid phase and polymer oxidations—manifests the crucial importance of molecular dynamics for both magnitude and sign of the one-step enrichment coefficient α(^{17}O). Molecular dynamics controls the spin selectivity of the two isotope-sorting reactions, chain propagation and chain termination, as well as their relative contribution into the overall isotope selection: the former dominates in nonviscous solutions, whereas the latter has an advantage in viscous systems with strongly retarded molecular motions.

A quantitative theory of the oxygen MIE and CIE has been developed and the equations for isotope enrichment as a function of oxygen conversion have been derived recently.[38e] The ratio of the radical addition rate constants $k_a(^{17}O^{16}O)/k_a(^{16}O^{16}O)$ for alkyl radicals from ethylbenzene is found to be 1.011, i.e. $^{17}O^{16}O$ molecules react, owing to MIE, by 1.1% faster than $^{16}O_2$ molecules. In contrast, the ratio of the rate constants $k_a(^{18}O^{16}O)/k_a(^{16}O^{16}O)$ for the same alkyl radical is 0.990, i.e. $^{18}O^{16}O$ molecules react by 1% slower than $^{16}O_2$ molecules. The ratio of the chain termination rate constants $k(RO^{17}O + {}^{16}OOR)/k(RO^{16}O + {}^{16}OOR)$ is found to be 1.8 ± 0.1 for the polymer oxidation.[38e]

Recently a strong isotope effect has been observed in the high temperature (350−400 °C) oxidation of polyaromatic polymers, polypyrromellitimide, and polyphenylquinoxaline, by molecular oxygen: the oxygen remainder appears to be enriched with ^{18}O ($\alpha \approx 1.003-1.006$) and impoverished with ^{17}O ($\alpha \approx 0.984-0.996$).[39] The kinetic arguments (no autocatalysis in oxygen consumption, no effect of inhibitors on the oxydation rate), as well as the composition and yield of reaction products compell us to discard the standard radical chain mechanism of oxidation and to accept the interaction of energetically low lying and, therefore, thermally accessible excited triplet states of aromatic fragments of macromolecules with molecular oxygen as a primary stage of oxidation process. Generating endoperoxides in singlet state, this reaction is spin selective since among the nine spin states of the pair of two triplets only one is allowed for the reaction. ^{17}O HFI in molecular oxygen is supposed to induce transformation of spin states and opens additional channels for the reaction of oxygen labeled by ^{17}O, providing the additional leakage of ^{17}O into the reaction products.[39]

It would be dishonest to hide a question why HFI in oxygen molecule, rather minor in comparison with intramolecular dipolar interaction or with strong electron spin relaxation, is still operating and influences the spin dynamics of such pairs as ($R^{\bullet}$ O_2) or

($T O_2$). This problem holds a mystery and is open for the theoretical inspection.

C. $^{28}Si/^{29}Si/^{30}Si$ Triad

The ^{29}Si MIE has been discovered by Step *et al.*[22] in the photolysis of silyl-containing ketone $PhCH_2COSi(CH_3)_2Ph$ in Triton X-100 micelles. As established by CIDNP, both direct and triplet-sensitized photolysis occur via radical pair mechanism similar to that of DBK photolysis, i.e.

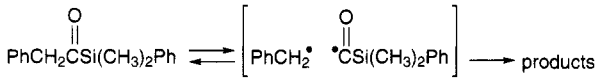

Direct photolysis starts from the excited singlet state of ketone molecule which generates RP in the singlet spin state. In contrast, triplet-sensitized photolysis proceeds through the generation of triplet RP, and this RP reaction pathway coexists with and even is strongly suppressed by the carbene mechanism, which involves the siloxycarbene insertion into the O–H bond of water molecules and amounts up to $^2/_3$ of total reaction probability.[21,22] In contrast, triplet-sensitized photolysis proceeds through the generation of triplet RP, and this RP reaction pathway coexists with and even is strongly suppressed by the carbene mechanism, which involves the siloxycarbene insertion into the O–H bond of water molecules and amounts up to $^2/_3$ of total reaction probability.[21,22]

In direct photolysis the starting silyl ketone is enriched with ^{13}C but the α coefficient is 1.032, the value typical for CIE and very close to α(CIE) for DBK photolysis. This is not an unexpected result since in the singlet RP ^{13}C MIE contributes almost nothing, at least not more than CIE. In triplet-sensitized photolysis α has been found to be much larger, 1.086. Taking into account that the triplet RP route constitutes only about $^1/_3$ and recalculating isotope enrichment according to this ratio (see eq 34) one can approximately estimate the total α value for ^{13}C as 1.26, which is not too different from that for DBK photolysis.

The silicon isotope enrichment as a function of ketone chemical conversion obeys eq 25 and is shown in Figure 16. The first important result derived from Figure 16 is that MIE-induced ^{29}Si enrichment in triplet-sensitized photolysis is higher than CIE-induced ^{30}Si enrichment: $\alpha(^{30}Si) = 1.005$, $\alpha(^{29}Si) = 1.023$. Again, taking into account the weight of RP route ($^1/_3$), one can estimate the total $\alpha(^{29}Si)$ value as 1.08 which is much higher than $\alpha(^{30}Si)$, but smaller than $\alpha(^{13}C)$. The reason for the relation $\alpha(^{29}Si) < \alpha(^{13}C)$ is that the HFI constant $a(^{13}C)$ in $COSi(CH_3)_2Ph$ radical is expected to be larger than $a(^{29}Si)$ and, therefore, ^{13}C contributes to the triplet–singlet conversion more than ^{29}Si ensuring in the predominance of ^{13}C MIE over ^{29}Si MIE.

The second impressive observation illustrated by Figure 16 is that the inversion in the spin multiplicity of RP in direct and sensitized photolysis is accompanied by the inversion of ^{29}Si MIE sign: ^{29}Si enrichment in the latter is replaced by small but reliably measurable impoverishment in the former. Noteworthy, ^{30}Si enrichment is not sensitive to the spin multiplicity of the RP precursor, the fact proving its CIE origin.

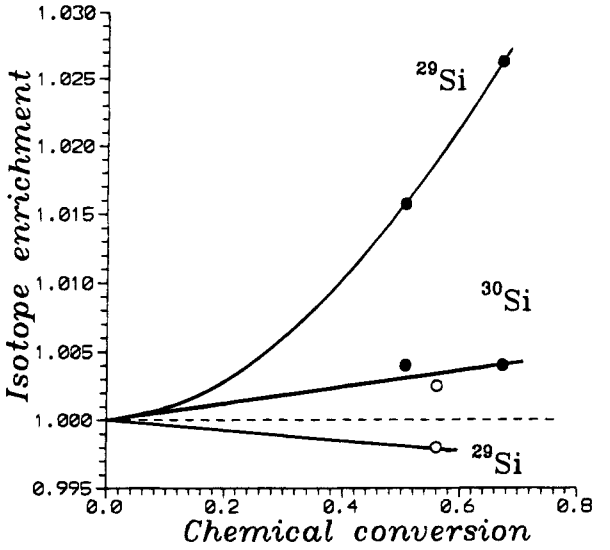

Figure 16. ^{29}Si and ^{30}Si isotope enrichment as a function of chemical conversion in the direct (open circles) and sensitized (filled circles) photolysis of silyl ketone.[22]

D. $^{32}S/^{33}S/^{34}S$ Triad

The ^{33}S MIE was observed by Step *et al.*[40] for the first time in 1990 in the direct photolysis of sulfur-containing ketone in SDS micelles. The reaction has been proved by CIDNP to occur through RP in triplet spin state according to the scheme:

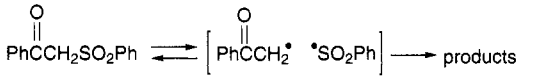

The dependence of sulfur isotope enrichment of the starting ketone on the chemical conversion shown in Figure 17 is again nicely described by eq 25.

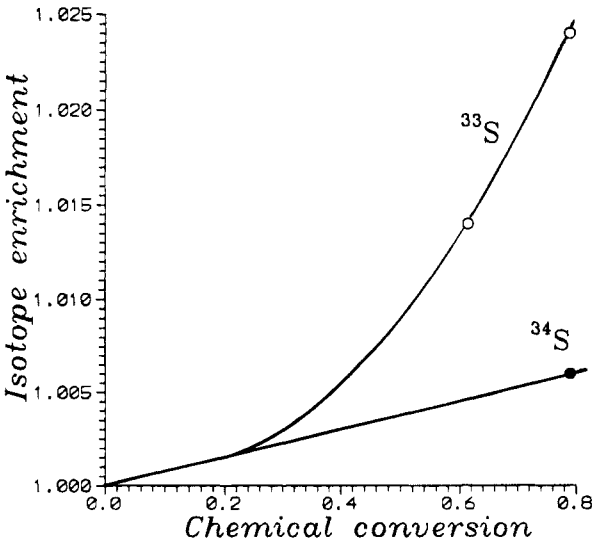

Figure 17. ^{33}S and ^{34}S isotope enrichment as a function of chemical conversion in the photolysis of sulfur-containing ketone.[40]

The superiority of ^{33}S MIE over the ^{34}S CIE is evident: $\alpha(^{33}S) = 1.015$, $\alpha(^{34}S) = 1.008$. In favor of MIE, it is worth mentioning that the CIE for ^{34}S is expected to be nearly twice as large as that for ^{33}S.

However, MIE-induced ^{13}C enrichment [$\alpha(^{13}C) = 1.04$] is rather small being comparable with that induced by CIE, since the HFI constants for ^{13}C in radical partners, $PhCOCH_2$ and $PhSO_2$, are too low (in comparison with $a(^{33}S) = 83$ G in $PhSO_2$ radical[41]) to contribute significantly into the ^{13}C nuclear spin selection.

E. $^{235}U/^{238}U$ Dyad

The perceptive reader has noticed the aspiration of the MIE researches to the heavier nuclei—^{13}C, ^{17}O, ^{29}Si, ^{33}Si. The reason is that an increase in mass is accompanied by an increase of spin–orbit coupling (SOC) which competes with HFI and causes the leakage of triplet–singlet conversion through the SOC. The leakage should diminish or even completely destroy MIE since in this case the electron spin system is coupled strongly not with the nuclear spins, as required for the MIE, but with the electron orbital momentum.

However, in the sequence of elements, for which MIE has been observed, the values of MIE have been changed only slightly although the SOC constants increase from 28 cm^{-1} for carbon to 382 cm^{-1} for sulfur, i.e. by more than an order of magnitude.[42] It means that the danger of a harmful SOC effect may be exaggerated, and one can take the risk of proceeding directly to a search of MIE for very heavy nuclei, from which uranium is the most attractive.

The search of uranium MIE requires solution of three problems: (i) to find the reactions of uranium compounds which would generate paramagnetic intermediates, spin carriers; (ii) to find spin selective steps in reactions of these intermediates; and (iii) to study the distribution of isotopes in the reaction products.

The last of these problems is the most risky, since there is no guarantee that the outer unpaired electron in uranium intermediate is able to break through the thick shell containing more than 90 electrons in order to reach the uranium nucleus and produce the large HFI energy required to ensure efficient nuclear spin selectivity.

Among many reactions of uranium compounds the photoreduction of uranyl salts which is known to involve the paramagnetic uranoyl ion UO_2^+ has been chosen. According to much chemical evidence the photochemical reactions of the uranyl ion UO_2^{2+} resemble those of triplet benzophenone although the spin multiplicity of the excited uranyl ion has been uncertain.

Three sets of experiments have reliably identified spin state multiplicity of excited uranyl ion UO_2^{2+} and, therefore, spin multiplicity of RP generated by the reactions of this ion. They are the CIDNP induced by photoreduction of uranyl ion by phenols[43] and benzylic acid,[44] a magnetic field effect in the polymerization of diallyl[(isopropylcarboxy)methyl]-methylammonium chloride photosensitized by uranyl ion,[45] and, at last, the nitroxyl radical CIDEP generated by transfer of electron spin polarization from excited UO_2^{2+} to nitroxyl radicals.[46] All these observations demonstrate unambiguously that photoexcited uranyl has a triplet spin multiplicity, and uranyl ion UO_2^+ takes part in spin-selective, nuclear spin-sorting reactions.[47]

Scheme 9

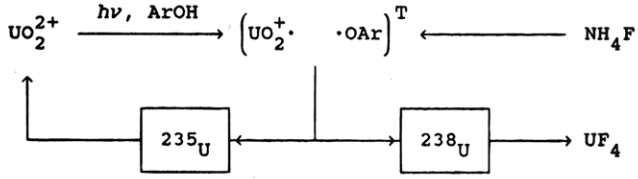

The photolysis of dioxouranium(VI) salts in water solutions as well as in SDS micelles[48] in the presence of substituted phenols (and NH_4F to precipitate U^{4+} ions) has been shown to yield unusual uranium isotope redistribution between the remainder of dioxouranium salt and reaction product UF_4: the former is enriched with light (magnetic) isotope nuclei, the latter is enriched with heavy (nonmagnetic) ones. It means that the molecules with the heavier isotope are more reactive (in contrast to CIE propensity) and implies the dominant role of MIE-induced isotope sorting. Scheme 9 shows the sequence of uranyl spin-selective reactions, responsible for the nuclear sorting.

In the photolysis of uranyl perchlorate salt $UO_2(ClO_4)_2$ in a D_2O micellar SDS solution in the presence of 2,6-diphenyl-4-stearoylphenol $\alpha(^{235}U)$ was found to be 1.020, while $\alpha(^{238}U) = 0.994$.[48] Therefore, being greater and opposite in sign to CIE, MIE again demonstrates its superiority over CIE even for uranium isotope nuclei.

The uranium MIE was also confirmed by Rykov *et al.*:[49] the photolysis of uranyl succinate containing 30% of ^{235}U in methanol-d_4 at the 85–90% conversion has resulted in the enrichment of the starting compound with ^{235}U isotope by 6%.

F. MIE vs CIE: Quantitative Summary

Figure 18 summarizes the α values for all magnetic isotope effects discovered up to this point in time. It provides a clear and pictorial demonstration of the quantitative scales of magnitudes of the magnetic and classical isotope effects.

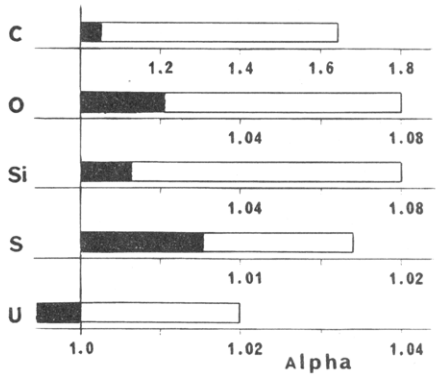

Figure 18. One-step enrichment coefficients α. The white fields indicate the range of α values for the magnetic isotope effects in isotopic pairs $^{13}C/^{12}C$, $^{17}O/^{16}O$, $^{29}Si/^{28}Si$, $^{33}S/^{32}S$, $^{235}U/^{238}U$. Black fields characterize classical isotope effects α(CIE) for isotopic pairs $^{13}C/^{12}C$, $^{18}O/^{16}O$, $^{30}Si/^{28}Si$, $^{34}S/^{32}S$, $^{235}U/^{238}U$, respectively. The values of α(CIE) are experimentally measured or estimated approximately as a square root of isotope mass ratios.

VII. Does Maximum of MIE Exist?

The CIE-induced isotope selectivity is well-known to be confined by the isotope mass ratio, which

restricts the range of permissible CIE magnitudes (providing that quantum tunneling is excluded from the consideration). As shown in the previous section, the MIE-induced selectivity is ordinarily much higher, so that MIE-induced isotope enrichment may be 1 or 2 orders of magnitude greater than that induced by CIE. The questions arise: is there a limit of MIE-induced isotope selection, and, if it exists, what is the ultimate selection, what is the highest MIE value?

The one-step enrichment coefficient α_G in eqs 25–28 is defined by eq 24 as the ratio $(1 - P)/(1 - P^*)$. The extreme α_G value is achieved under condition $P = 0$, $P^* = 1$ which implies that only magnetic RPs necessarily recombine and regenerate the molecules with magnetic nuclei, whereas the nonmagnetic RPs are strictly locked for the reaction. Therefore, α(MIE) goes to infinity and eq 25 can be easily transformed into

$$S = (1 - F)^{-1} \tag{51}$$

where S is the isotope enrichment and F is the total chemical conversion. It defines the top nuclear spin selectivity which is realized in such a regime of chemical reaction when only molecules with nonmagnetic isotope nuclei react and decompose, while the molecules with magnetic nuclei remain intact. In other words, this regime is equivalent to chemically induced isotope "purification".

Now we formulate the routes to achieve the largest MIE.

(i) The first problem to be solved is to direct the chemical reaction along the pathways with paramagnetic intermediates (radicals, in particular) to accomodate the chemistry to spin-selective chemical stages.

(ii) High reversibility of the spin-selective reaction makes it possible for the molecules to undergo many repetitive spin selective and, therefore, isotopically selective events. It results in highly efficient isotope separation in the microreactors of confined geometry (micelles, zeolite and porous glass cavities, etc.). The best selectivity is attained if the characteristic time of triplet–singlet conversion and the diffusional lifetime of the magnetic RP are comparable. It ensures that preferrably magnetic RPs are able to experience the triplet–singlet conversion and reencounter during the RP lifetime.[50]

(iii) To guarantee large MIE it is necessary to modify the reaction mechanism so that the spin-selective process would occur in triplet spin state. This is the reason, in particular, why the triplet-sensitized photolysis is preferably used to enhance MIE.

(iv) A large HFI is a necessary but not sufficient condition to guarantee MIE of high magnitude. The spin-selective birth of molecule in radical pair is a result of the collective efforts and coordinated choreography (according to Turro's expression) of all three dynamics—spin, molecular, and chemical, so that the synchronism of these dynamics provides a physically favorable condition for the nuclear spin selection. The ^{17}O MIE in chain oxidation processes considered in section VI.B illustrates this statement: the molecular dynamics strongly influences the MIE magnitudes, moreover, it may change the priority of competitive spin selective reactions in isotope separation: the recombination of peroxy radicals in polymers versus addition of alkyl radicals to molecular oxygen in liquids.

(v) A new way to enhance the MIE and MIE-induced isotope separation is the selective microwave pumping of triplet radical pairs with magnetic nuclei which accelerates their spin conversion and stimulates the selective regeneration of "magnetic" molecules only. The idea of the microwave-induced MIE was formulated in 1981[51a] and embodied in 1991 experimentally.[51b] The combination of two microwave actions is expected to be even more promising: the low-amplitude microwave pumping of magnetic RPs, which accelerates their spin conversion, and the high-amplitude microwave pumping of nonmagnetic pairs, which retards or even locks their spin conversion preventing their recombination. Such a combination may provide the most favorable conditions for the isotopically selective microwave-stimulated spin dynamics.[1b]

The main obstacles on the way to the highest MIE are the leakages of two sorts. MIE is a result of the spin conversion induced by HFI; however, HFI is far from being the only magnetic interaction which contributes to spin conversion. Spin–orbit and spin–rotational couplings as well as dipolar electron interaction provoke electron spin relaxation. The spin conversion caused by these non-Fermi interactions competes with that stimulated by Fermi interaction. This additional non-Fermi concurrent spin conversion channel is a spin leakage because it does not influence the nuclear spin subsystem and, hence, does not produce MIE. This kind of spin conversion induced by non-Fermi interactions (dipolar, spin–orbit, spin–rotational, etc.) can be referred to as physical leakage. Even the HFI itself can be counterproductive to magnetic isotope enrichment. If the target is a specific element, other magnetic nuclei in the radicals (usually ^1H) will decrease the MIE for the desired element and provoke a physical leakage.

The chemical leakage is even more destructive for the MIE. First of all, intra-RP reactions, which are competitive with the key nuclear spin-selective reaction, result in the spreading of magnetic isotope nuclei among the different species and prevent their accumulation, their concentration in a single product. For instance, in the series of ketones listed below the one-step ^{13}C enrichment coefficient α decreases as the yield χ of benzaldehyde (the product of disproportionation reaction in the radical pair) increases:[52]

	α	χ
$PhC(O)CH_2Ph$	1.40	0
$PhC(O)CH(CH_3)Ph$	1.20	23
$PhC(O)C(CH_3)_2Ph$	1.15	41

Evidently, inclusion of only one intrapair reaction in addition to pair recombination strongly decreases the efficiency of ^{13}C accumulation in the recovered ketone molecules. For the same reason (namely, competition of the recombination with other reactions), ^{13}C isotope enrichment in the photolysis of cyclic ketones appears to be rather low ($\alpha \approx 1.03$–1.06) even if the spin dynamics is the limiting factor in the recombination of biradical termini, although from the viewpoint of the chain and chemical dynamics the corresponding biradicals seem to be almost

ideal molecular systems to promote efficient nuclear spin selection.

The competition of radical and nonradical mechanisms of the reaction is the second source of the chemical leakage since the nonradical channel partly eliminates the reaction from the spin-selective process (section II.C). The competition of two radical pathways, each of which starts from the radical pairs with different spin state multiplicity, directs the spin evolution of the pairs oppositely and cancels the nuclear spin selectivity, at least partly, also suppressing MIE.

VIII. MIE: Known and Unknown

Now it is perfectly clear that the new isotope effect is an outstanding phenomenon so that its discovery is likely one of the important events in modern chemistry. In contrast to the well-known classical isotope effect, which selects the nuclei according to their mass, the magnetic isotope effect sorts and directs isotopic nuclei into the different reaction products according to the nuclear spins and magnetic moments. It results in the fractionation of magnetic and nonmagnetic nuclei in chemical, biochemical, geochemical, and cosmochemical processes and provides an easily controlled way of highly efficient isotope separation.

This review demonstrates that the main fundamental problems of the MIE physics and chemistry are now solved, the foundations of the theory are formulated and experimentally proved. However, many questions remain unanswered. The key to the control of the nuclear spin selectivity and MIE is an integrated spin dynamics combined with molecular and chemical dynamics. The problem is not only to ensure comfortable conditions for the spin evolution (strong electron–nuclear magnetic interactions, optimal lifetimes of the spin selective reaction partners, favorable molecular dynamics, selective microwave pumping, disengagement of the spin leakage through the non-Fermi interactions, etc.). It is even more important to organize the chemistry so as to conform the chemical reaction to predetermined physics, i.e. to direct the reaction through the paramagnetic intermediates, to create the required pairs of these species, to prepare a favorable starting spin multiplicity of these pairs. General principles of such organization are known, but for many particular chemical situations the solution of these problems is not yet found. As an illustration, one can appeal to unsuccessful attempts to observe MIE for tin and mercury nuclei.

One more important issue, the behavior of the exchange potential along the chemical bond at large distances, is equivalent to the magnetic probing of the reaction dynamics trajectories and transition state radiospectroscopy.[19] On the other side, the exchange potential behavior regulates the relative contributions of the adiabatic passage of the S–T term crossing (where $J = a$) and free spin motion (at $J = 0$) into the nuclear spin selectivity and MIE. These and some other problems which have been mentioned in the review are yet to be solved. In any case, it is clear that the problems of nuclear spin selectivity control are equivalent to the general problems of the regulation of the reaction physics and chemistry. And this fine science is now in fast progress.

IX. Acknowledgments

The author is grateful to his colleagues V. F. Tarasov, E. N. Step, I. V. Khudyakov, L. L. Yasina, I. A. Shkrob from the Institute of Chemical Physics (Moscow) for their fruitful and friendly long-term collaboration which resulted in the experimental discovery of all magnetic isotope effects presently known. Special gratitude to Professor N. J. Turro for his inspiring discussions and friendly support of scientific cooperation between Columbia University and Institute of Chemical Physics. The reviewers deserve particular author's gratitude for their careful and professional inspection and correction of the manuscript. The financial support by the Russian Fund for Fundamental Research (Grant 93-3-5227) is also acknowledged.

X. References

(1) (a) Salikhov, K. M.; Molin, Yu. N.; Sagdeev, R. Z.; Buchachenko, A. L. *Spin Polarization and Magnetic Effects in Radical Reactions*; Elsevier: Amsterdam, 1984. (b) Buchachenko, A. L.; Frankevich, E. L. *Chemical Generation and Reception of Radio- and Microwaves*; VCH Publishers: New York, 1993. (c) *Chemically Induced Magnetic Polarization*; Lepley, A. R., Closs, G. L., Eds.; London: Wiley, 1973.
(2) (a) Buchachenko, A. L. *Progr. React. Kinet.* **1984**, *13*, 163. (b) Gould, I. R.; Turro, N. J.; Zimmt, M. B. *Adv. Phys. Org. Chem.* **1984**, *20*, 1. (c) McLauchlan, K.; Steiner, U. **1991**, *73*, 241. (d) Turro, N. J.; Krauetler, B. In *Diradicals*; Borden, W. T., Ed.; Wiley: New York, 1982. (e) Buchachenko, A. L. *Russ. J. Phys. Chem.* **1977**, *51*, 1445.
(3) Buchachenko, A. L. *Russ. Chem. Rev.* **1993**, *62*, 1139–1149.
(4) Step, E. N.; Buchachenko, A. L.; Turro, N. J. *J. Org. Chem.* **1992**, *57*, 7018.
(5) (a) Steiner, U.; Ulrich, T. *Chem. Rev.* **1989**, *89*, 51. (b) Freed, J. H.; Pedersen, J. B. *Adv. Magn. Res.* **1976**, *8*, 1.
(6) Noyes, R. M. *J. Chem. Phys.* **1954**, *22*, 1349.
(7) Razi Naqvi, K.; Mork, K. J.; Waldenstrom, S. *J. Phys. Chem.* **1980**, *84*, 1315.
(8) Deutch, J. M. *J. Chem. Phys.* **1972**, *56*, 6076.
(9) Mozumder, A. *J. Chem. Phys.* **1968**, *48*, 1659.
(10) Sterna, L.; Ronis, D.; Wolfe, S.; Pines, A. *J. Chem. Phys.* **1980**, *73*, 5493.
(11) Tarasov, V. F.; Buchachenko, A. L. *Russ. J. Phys. Chem.* **1981**, *55*, 1921.
(12) den Hollander, J. A. *Chem. Phys.* **1975**, *10*, 167.
(13) Belyakov, V. A.; Buchachenko, A. L. *Russ. J. Chem. Phys.* **1983**, *1385*, 1510.
(14) (a) Buchachenko, A. L.; Galimov, E. M.; Ershov, V. V. *Dokl. Akad. Nauk SSSR* **1976**, *228*, 379. (b) Sagdeev, R. Z.; Leshina, T. V.; Kamkha, M. A.; Belchenko, O. I.; Molin, Y. N.; Rezvukhin, A. J. *Chem. Phys. Lett.* **1977**, *48*, 89.
(15) Lawler, R. G.; Evans, G. T. *Ind. Chim. Belge* **1971**, *36*, 1087.
(16) Buchachenko, A. L.; Pershin, A. D. Unpublished results. Benzene, the product of benzoyl peroxide thermolysis (80 °C, conversion ~70–80%) was enriched by 1.2%.
(17) Bernstein, R. *J. Phys. Chem.* **1952**, *56*, 893. In this paper, "classical isotope effect" is used to denote all mass-dependent isotope effects, not just the high-temperature limit of the isotope effect as in the standard definition.
(18) Tarasov, V. F. *Russ. J. Phys. Chem.* **1980**, *54*, 2438.
(19) Buchachenko, A. L.; Tarasov, V. F.; Ghatlia, N. G.; Turro, N. J. *Chem. Phys. Lett.* **1992**, *192*, 139.
(20) Step, E. N.; Tarasov, V. F.; Buchachenko, A. L. *Russ. J. Gen. Chem.* **1985**, *55*, 2348.
(21) Step, E. N.; Tarasov, V. F.; Buchachenko, A. L. *Bull. Acad. Sci. USSR, Div. Chem. Sci.* **1988**, *37*, 2024.
(22) Step, E. N.; Tarasov, V. F.; Buchachenko, A. L. *Chem. Phys. Lett.* **1988**, *144*, 523.
(23) Tarasov, V. F.; Askerov, D.; Buchachenko, A. L. *Bull. Acad. Sci. USSR, Div. Chem. Sci.* **1982**, *31*, 1786.
(24) (a) Kraeutler, B.; Turro, N. *Chem. Phys. Lett.* **1980**, *70*, 266. (b) Turro, N.; Anderson, D.; Kraeutler, B. *J. Am. Chem. Soc.* **1982**, *103*, 3892. (c) Turro, N.; Kraeutler, B. *J. Am. Chem. Soc.* **1978**, *100*, 7432.
(25) Tarasov, V.; Buchachenko, A. L. *Bull. Acad. Sci. USSR, Div. Chem. Sci.* **1983**, *32*, 68.

(26) Step, E. N.; Buchachenko, A. L.; Turro, N. J. *Chem. Phys. Lett.* **1991**, *186*, 405.
(27) Tarasov, V. F.; Shkrob, I. A.; Step, E. N.; Buchachenko, A. L. *Chem. Phys.* **1989**, *135*, 391.
(28) Tarasov, V. F.; Ghatlia, N. D.; Buchachenko, A. L.; Turro, N. J. *J. Phys. Chem.* **1991**, *95*, 10220.
(29) Turro, N. J.; Chow, M.-F.; Chung, C.-J.; Weed, G. C.; Kraeutler, B. *J. Am. Chem. Soc.* **1980**, *102*, 4843.
(30) Tarasov, V. F.; Buchachenko, A. L. *Bull. Acad. Sci. USSR, Div. Chem. Sci.* **1983**, *32*, 72.
(31) Turro, N. J.; Anderson, D.; Kraeutler, B. *Tetrahedron Lett.* **1980**, *21*, 3.
(32) Buchachenko, A. L. *Bull. Russ. Acad. Sci., Div. Chem. Sci.* **1995**, *44*, 1639.
(33) (a) Kraeutler, B.; Turro, N. J. *Chem. Phys. Lett.* **1980**, *70*, 270. (b) Turro, N. J.; Chow, M. F.; Kraeutler, B. *Chem. Phys. Lett.* **1980**, *73*, 545.
(34) Buchachenko, A. L.; Tarasov, V. F. *Russ. J. Phys. Chem.* **1981**, *55*, 1649.
(35) Step, E. N.; Tarasov, V. F.; Buchachenko, A. L.; Turro, N. J. *J. Phys. Chem.* **1993**, *97*, 363.
(36) Shida, T. *J. Phys. Chem.* **1975**, *82*, 991.
(37) Tarasov, V. F.; Ghatlia, N. D.; Buchachenko, A. L.; Turro, N. J. *J. Am. Chem. Soc.* **1992**, *114*, 9517.
(38) (a) Belyakov, V. A.; Galimov, E. M.; Buchachenko, A. L. *Dokl. Acad. Nauk USSR* **1978**, *243*, 924. (b) Buchachenko, A. L.; Fedorov, A. V.; Yasina, L. L.; Galimov, E. M. *Chem. Phys. Lett.* **1984**, *103*, 405. (c) Yasina, L. L.; Buchachenko, A. L. *Chem. Phys. Lett.* **1990**, *146*, 225. (d) Turro, N. J.; Chow, M.-F. *J. Am. Chem. Soc.* **1980**, *102*, 1190. (e) Buchachenko, A. L.; Yasina, L. L.; Belyakov, V. A. *J. Phys. Chem.* **1995**, *99*, 4240.
(39) Buchachenko, A. L.; Yasina, L. L. *Bull. Russ. Acad. Sci., Div. Chem. Sci.* **1994**, *43*, 1328.
(40) Step, E. N.; Tarasov, V. F.; Buchachenko, A. L. *Nature* **1990**, *345*, 25.
(41) Geoffroy, M.; Lucken, E. *J. Chem. Phys.* **1971**, *55*, 2719.
(42) Khudyakov, I. V.; Serebrennikov, Yu. A.; Turro, N. J. *Chem. Rev.* **1993**, *93*, 537.
(43) Buchachenko, A. L.; Khudyakov, I. V.; Klimchuk, E. S.; Margulis, L. A. In *Organic Free Radicals*; Fischer, H., Ed.; Springer: Berlin, 1988.
(44) Buchachenko, A. L.; Khudyakov, I. V.; Klimchuk, E. S.; Margulis, L. A. *J. Photochem. Photobiol.* **1989**, *46*, 281.
(45) Golubkova, N.; Khudyakov, I.; Topchiev, D.; Buchachenko, A. *Dokl. Akad. Nauk* **1988**, *300*, 147.
(46) Khudyakov, I. V.; Turro, N. J. *Res. Chem. Intermed.* **1993**, *19*, 15.
(47) (a) Buchachenko, A. L.; Khudyakov, I. V. *Russ. Chem. Rev.* **1991**, *60*, 555. (b) Buchachenko, A. L.; Khudyakov, I. V. *Acc. Chem. Res.* **1991**, *24*, 177.
(48) Khudyakov, I. V.; Buchachenko, A. L. *J. Chem. Soc. Mendeleev Commun.* **1993**, *3*, 135.
(49) Rykov, S. V.; Khudyakov, I. V.; Skakovsky, E. D.; Tychinskaya, L. Yu.; Ogorodnikova, M. M. *J. Photochem. Photobiol. A* **1992**, *66*, 127.
(50) Tarasov, V. F.; Buchachenko, A. L.; Maltsev, V. I. *Russ. J. Phys. Chem.* **1981**, *55*, 1921.
(51) (a) Buchachenko, A. L.; Tarasov, V. F. *Russ. J. Phys. Chem.* **1981**, *55*, 936. (b) Tarasov, V. F.; Bagryanskaya, E. G.; Grishin, Y. A.; Sagdeev, R. Z.; Buchachenko, A. L. *J. Chem. Soc. Mendeleev Commun.* **1991**, *1*, 85.
(52) Tarasov, V. F.; Step, E. N.; Margulis, L.; Buchachenko, A. L. *Bull. Acad. Sci. USSR, Div. Chem. Sci.* **1989**, *38*, 221.

CR9400166